MATERIALS CHEMISTRY
FRONTIERS

REVIEW

View Article Online
View Journal | View Issue

Cite this: *Mater. Chem. Front.*, 2024, **8**, 2322

Recent advances in vacuum- and laser-based fabrication processes for solar water-splitting cells

Jinhyeong Kwon, †[a] Seonmi Ko,†[b] Hyeonwoo Kim,[b] Hyo Jin Park,[b] Changwook Lee[b] and Junyeob Yeo *[bc]

Received 29th December 2023,
Accepted 9th April 2024

DOI: 10.1039/d3qm01336g

rsc.li/frontiers-materials

The demand for zero-emission energy sources has recently intensified, driven by growing concerns over global warming and climate change. Among various renewable energy technologies, solar water-splitting cells have emerged as a promising avenue for harnessing hydrogen energy by exciting photo-carriers. These cells are typically fabricated using vacuum-based techniques such as physical vapour deposition, atomic layer deposition, chemical vapour deposition, and sputtering. Although these methods deliver moderate performance, they are characterised by extensive production steps and significant costs. This review examines the current vacuum-based fabrication processes for solar water-splitting cells and explores advanced or alternative techniques, with a particular emphasis on optical methods, especially laser processing, for fabricating these cells.

[a] *Laser-processed Nanomaterials Engineering Lab., Research Institute of Sustainable Development Technology, Korea Institute of Industrial Technology (KITECH), 89 Yangdaegiro-gil, Ipjang-myeon, Seobuk-gu, Chungchengnam-do, Cheonan, 31056, Republic of Korea*

[b] *Novel Applied Nano Optics (NANO) Lab, Department of Physics, Kyungpook National University, 80 Daehak-ro, Buk-gu, Daegu, 41566, Republic of Korea. E-mail: junyeob@knu.ac.kr*

[c] *Department of Hydrogen & Renewable Energy, Kyungpook National University, 80 Daehak-ro, Buk-gu, Daegu, 41566, Republic of Korea*

† These authors contributed equally to this work.

1. Introduction

The world is grappling with an environmental crisis due to global climate change, which leads to severe repercussions for the planet. These include air pollution,[1] species extinction,[2] extreme weather events,[3] and global warming,[4,5] all resulting from the disruption of the natural balance. Among these, global warming is a significant driver of climate change, primarily due to the emissions of greenhouse gases (GHGs) from the

Jinhyeong Kwon

Dr. Jinhyeong Kwon serves as a senior researcher at the Korea Institute of Industrial Technology (KITECH) in Cheonan, Korea. He earned his PhD in 2014 from KAIST, Korea. His research at KITECH is distinguished by his dedication to advancing laser-based manufacturing processes, alongside pioneering developments in the domains of energy and electronics. His notable contributions encompass the enhancement of metal oxide-based water-splitting photoelectrochemical cells, the innovation in flexible optoelectronics, and the advancement of wearable sensors. Currently, his research interests are directed toward the laser processing of nanomaterials for innovative solar-driven water-splitting solar cells, photothermal desalination, and flexible electrochromic devices.

Seonmi Ko

Ms. Seonmi Ko is currently a PhD student in the Department of Physics at Kyungpook National University, Republic of Korea, under the supervision of Prof. Junyeob Yeo. Her research interests are plastic decomposition and wastewater treatment by using photoelectric catalysts. Her current research is on the fabrication of photoanodes based on transition metal oxides via laser processing for water splitting photoelectrochemical (PEC) cells.

combustion of fossil fuels such as coal, oil, and gas.[6–9] These sources are responsible for 75% of global GHG emissions and nearly 90% of carbon dioxide emissions.[7] Consequently, the development of clean and sustainable energy sources is receiving heightened focus, with significant efforts directed toward reducing and replacing fossil fuels. Consequently, hydrogen emerges as a viable, clean energy source for generating electricity through hydrogen fuel cells, which uniquely emit water as a byproduct.[10] Hydrogen boasts an energy density of 142 kJ g^{-1}, tripling that of natural gas and quadrupling that of gasoline.[11] As a secondary energy source, akin to electricity and gasoline, hydrogen is produced from the conversion of primary energy sources, including both fossil fuels and renewable sources.[12,13] Secondary energy sources, due to their convenience in storage and transport in gas or liquid form, find extensive use across various industrial, commercial, and residential applications.

Hydrogen can be sourced from plentiful water or fossil fuels, with the production methods categorised into grey, blue, and green hydrogen routes.[14–16] Grey hydrogen is produced through the catalytic chemical reactions between methane, the primary component of natural gas, and high-temperature steam. This process yields hydrogen and carbon dioxide, with approximately 10 kg of carbon dioxide emitted for every 1 kg of hydrogen produced. Blue hydrogen utilises the same production process as grey hydrogen but incorporates carbon capture and storage (CCS) technology to capture and sequester the carbon dioxide generated during production rather than releasing it into the atmosphere.[16] This makes blue hydrogen more environmentally friendly than grey hydrogen, resulting in lower carbon dioxide emissions. The CCS technology is relatively mature and competitive, positioning blue hydrogen as the most practical alternative, though it does not completely eliminate carbon dioxide emissions. Green hydrogen, in contrast, is generated by electrolysing water using electrical energy derived from renewable sources, such as solar or wind power, to separate water into hydrogen and oxygen.[17] Therefore, it is

Hyeonwoo Kim

Mr. Hyeonwoo Kim is currently a PhD student in the Department of Mechanical Engineering at Korea Advanced Institute of Science & Technology (KAIST). He obtained his MS and BS degrees from the Department of Physics at Kyungpook National University. His research interests include high-precision laser processing for flexible/stretchable electronics and energy devices (supercapacitors, green hydrogen harvesters, and batteries).

Hyo Jin Park

Ms. Hyo Jin Park is currently pursuing a master's degree in Prof. Junyeob Yeo's lab at the Department of Physics, Kyungpook National University, Republic of Korea. Her research interests lie in studying materiality and mechanism of nano-cathode materials in photoelectrochemical cells, and she is currently conducting research on control and restoration of efficiency degradation of photoreceptor devices through laser repair of transition metal oxide photoelectrodes.

Changwook Lee

Mr. Changwook Lee is currently pursuing MS in physics, Novel Applied Nano Optics lab, Kyungpook National University, Korea. He earned his BS in 2023 from KNU, Korea. His main research interests are fabrication of wearable photodetectors using semiconductor materials. Currently, besides conventional ultraviolet radiation detection, his research interests are the nanogenerator devices that are implemented in this way.

Junyeob Yeo

Prof. Junyeob Yeo is currently an associate professor in the Department of Physics/Department of Hydrogen & Renewable Energy at Kyungpook National University, Republic of Korea. He received his BS and MS degrees from the Department of Physics at Seoul National University and PhD degree from the Department of Mechanical Engineering at KAIST in 2013. Then, he worked as a postdoctoral researcher in the Department of Mechanical Engineering at UC Berkeley from 2014 to 2015. His research interests include laser nano-processing for wearable optoelectronics and renewable energy devices (PEC, supercapacitors, and nanogenerators) via study of light–matter interactions.

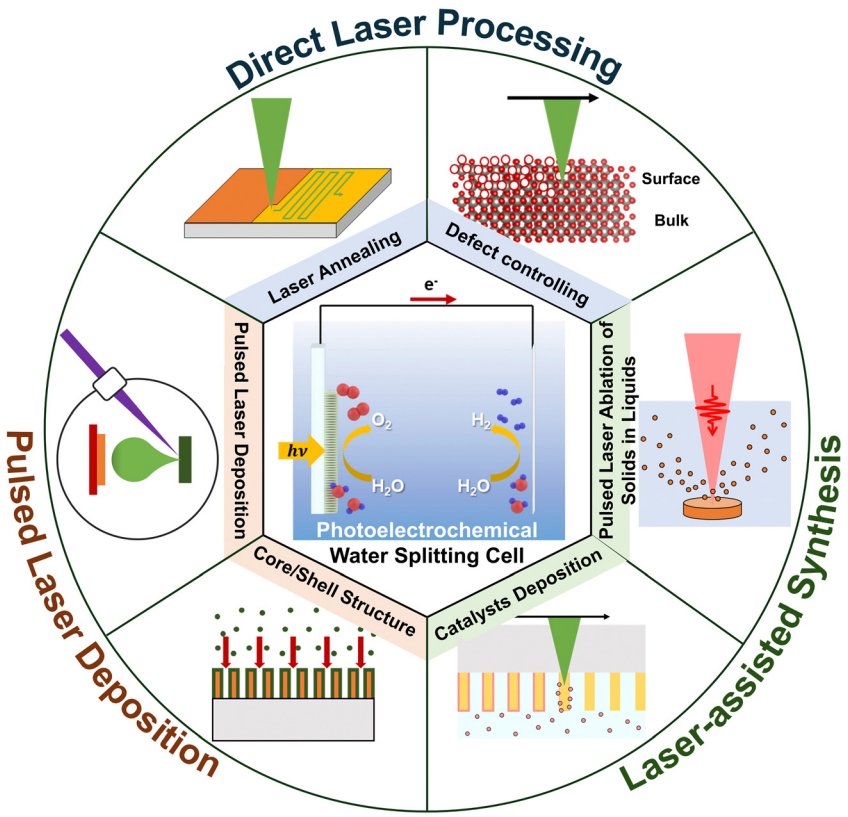

Fig. 1 Categorisation of laser-assisted fabrication processes for solar water-splitting cells.

regarded as the "ultimate environmentally friendly hydrogen" since it does not produce carbon dioxide emissions during its production. However, due to the high costs associated with renewable energy and the inefficiency of current electrolysis facilities, green hydrogen production costs are higher than grey hydrogen. Despite these challenges, numerous efforts are underway to transition to a green hydrogen society, including developing solar water-splitting cells.[18,19]

This review explores the manufacturing techniques of solar water-splitting cells, focusing on studies from 2020 to 2023. It begins with an overview of vacuum-based fabrication methods, prevalent in most manufacturing techniques, and introduces recent advancements in optical-based processes, especially those involving lasers (Fig. 1). This section underscores the innovative aspects of using lasers in manufacturing and explores potential future developments.

2. Basic science of solar water-splitting cells

Solar water-splitting cells harness solar energy to dissociate water molecules into hydrogen and oxygen gases through photoelectrochemical (PEC) reactions.[20,21] These processes depend on the interaction between a semiconductor material and an electrolyte, allowing light penetration and facilitating the reaction.[20,22] The selection of semiconductor materials is pivotal, as it directly affects the PEC reaction's efficiency through light absorption and the generation of photoexcited charge carriers. Prominent materials for photoanodes and photocathodes in PECs include metal-oxide semiconductors such as CdS,[23] CdSe,[24] CuO,[25,26] $BaTiO_3$,[27,28] $BiVO_4$,[29] $SrTiO_3$,[30] TiO_2,[31–34] WO_3,[35–37] and ZnO.[38–41]

Semiconductor materials typically absorb photons with energies exceeding their bandgaps, leading to the generation of electron–hole pairs. This absorption excites electrons from the valence band (VB) to the conduction band (CB), creating charge carriers while holes remaining in the VB. The excited electrons transition to the CB, becoming free electrons. These free electrons are then transferred to the working electrode (photoanodes for n-type semiconductor materials and photocathodes for p-type semiconductor materials),[42] as depicted in Fig. 2. The working electrode is typically modified with materials that facilitate water reduction to hydrogen gas ($2H_2O \rightarrow 2H_2 + 2e^-$). Simultaneously, holes in the VB migrate to the counter electrode, contributing to water oxidation and oxygen gas production ($2H_2O \rightarrow O_2 + 4H^+ + 4e^-$).[43] The gases generated can be harvested as renewable energy sources. Enhancing PEC efficiency involves surface modification to prevent electron–hole pair recombination.

The electrolyte completes the circuit in the solution by enabling ion flow between the electrodes. Its pH significantly influences PEC efficiency,[44] with H^+ and OH^- concentrations in the electrolyte critical for the acceleration of reduction or

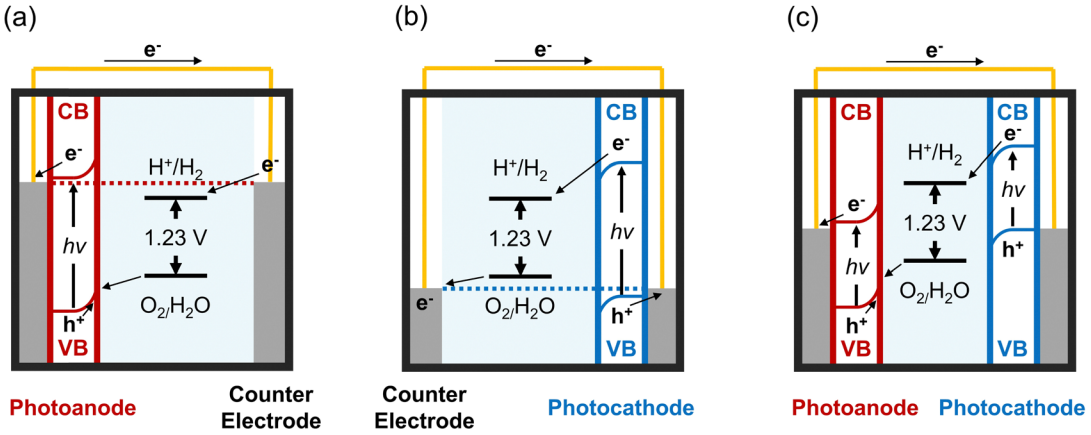

Fig. 2 Energy diagrams of solar water-splitting PEC cells for (a) photoanode, (b) photocathode, and (c) combined photoanode and photocathode configurations.

oxidation processes.[45,46] While numerous factors are at play, the selection of suitable materials and surface processing techniques is key to the overall efficiency of water-splitting PEC reactions. Consequently, substantial efforts focus on employing various nanoscale materials and precision processing tools to advance PEC technology.[47] Metal oxides with designed nanostructures are preferred, as nanomaterials offer significant benefits due to their size-dependent properties, including chemical, electrical, and optical characteristics, along with a high surface-to-volume ratio. Complex nanostructured designs provide ample sites for chemical reactions, reduce defects, and shorten electron–hole migration distances. This minimises electron–hole recombination and significantly boosts photoresponse efficiency.[48–50]

To enhance their surface area, nanomaterials have been intentionally designed in various forms and structures, such as thin films, porous frameworks, nature-mimicking branching systems, and hierarchical configurations. Among these, hierarchical metal-oxide nanostructures have garnered significant attention for electrochemical applications because of their straightforward core-and-shell structure. This has led to an increased focus on developing fabrication methods for the core materials.[51–53] Historically, vapour–liquid–solid processes, often conducted under vacuum conditions, were the primary methods for synthesising metal-oxide-based hierarchical nanostructures. However, recent studies have adopted hybrid fabrication techniques combining dry and wet methods to produce these complex structures.

3. General fabrication processes for solar water-splitting cells

The operational principle of solar water-splitting cells centres on efficient light absorption, effective charge separation, and controlled redox reactions at the electrodes. Current research aims to improve cell efficiency to make them more feasible for sustainable hydrogen production and energy storage solutions. The most advanced solar water-splitting cells are created using vacuum-based fabrication techniques, such as physical vapour deposition (PVD), chemical vapour deposition (CVD), and atomic layer deposition (ALD). These methods are essential for constructing and optimising the materials and components utilised in solar water-splitting cells. Comprehensive information on various solar water-splitting cells developed through vacuum-based processes is compiled in Table 1.

Table 1 Summarised data of the solar water-splitting cells fabricated by vacuum-based processes

Method	J_{max} (mA cm^{-2}) (at 1.23 V *vs.* RHE)	Material	Electrolyte	Ref.
MS-GLAD[a]	2.40 (at 1.0 V *vs.* Ag/AgCl)	WO_3/Ag_2S	0.5 M Na_2SO_4	57
Sputtering	4.00	$NiFeO_x/Ta_3N_5/Ta$	0.1 M Na_3PO_4	58
CVD	5.50 (at 1.2 V *vs.* SCE)	Branched ZnO	0.1 M Na_2SO_4	64
CVD	0.029 (at 1.2 V *vs.* SCE)	P doped ZnO	0.1 M Na_2SO_4	65
AACVD[b]	1.241	40 mol% Fe-doped MoS_2/Mo_2S_3	0.35 M Na_2SO_3 and 0.25 M Na_2S	66
PECVD[c]	9.00	RuO_x	1 M NaOH	67
CVD	0.78 (at 0.8 V *vs.* Ag/AgCl)	WO_3/Fe_2O_3	1 M NaOH	68
ALD	−3.71 (at 0 V *vs.* RHE)	Cu_2O/TiO_2/rGO/NiFe	0.5 M Na_3PO_4	73
ALD	W:$BiVO_4$ photoanode: ~1.23 (at 0.79 V *vs.* RHE) $CuBi_2O_4$ photocathode: 0.77 (at 0.67 V *vs.* RHE)	W:$BiVO_4$–$CuBi_2O_4$/CdS/TiO_2/RuO_x	0.3 M K_2SO_4 and 0.2 M KPi	74
ALD	—	WO_3/TiO_2	0.5 M Na_2SO_4	75
ALD	2.38	CdS@ZnO	0.1 M Na_2SO_4	76
ALD	0.0026 (at 0.6 V *vs.* NHE)	Hf–ZnO	0.5 M Na_2SO_4	77

[a] MS-GLAD: magnetron sputtering with glancing angle deposition. [b] AACVD: aerosol-assisted CVD. [c] PECVD: plasma-enhanced CVD.

3.1. PVD process

PVD utilises physical methods such as evaporation or sputtering to deposit materials onto substrates. This technique enables the creation of high-purity thin films and uniform coatings, significantly improving the durability and performance of photoelectrodes.[54] PVD can be conducted at relatively low temperatures, making it ideal for heat-sensitive substrates and materials. PVD systems are generally simpler, more cost-effective, and easier to operate and maintain. Overall, PVD is well-suited for applications requiring pure films and durable coatings, commonly found in electronics, optics, and the automotive industry.[55] Some recent studies of PVD-based fabrication methods (Fig. 3) for solar water-splitting cells are discussed below.

S. Limwichean *et al.* used magnetron sputtering with glancing angle deposition (MS-GLAD) and 2-h post-annealing in air to fabricate nanostructured WO_3 thin films with diverse morphologies.[56] The positioning of the substrate within the MS-GLAD setup significantly impacted the films' morphology, crystallinity, optical transmittance, and PEC performance. By adjusting substrate positions, the nanorod film layer of WO_3 could be precisely engineered, leading to enhanced PEC efficiency and demonstrating the potential of MS-GLAD in improving photoanodes for solar water-splitting cells. J. Yadav and J.P. Singh described a two-step method to create a WO_3/Ag_2S heterojunction to boost PEC performance. This involved depositing a WO_3 thin film *via* DC sputtering and forming well-separated Ag_2S nanorods using MS-GLAD.[57] The WO_3/Ag_2S heterojunction showed superior light absorption and a higher photocurrent density of 2.40 mA cm^{-2} (at 1.0 V Ag/AgCl) than the bare WO_3 thin film (0.34 mA cm^{-2}). The vertically tilted Ag_2S nanorods enhanced light trapping, and electrochemical impedance spectroscopy indicated low charge-transfer resistance at the semiconductor–electrolyte interface, reflecting a high flat band potential. This research underscored the importance of the interface between WO_3 and Ag_2S in water-splitting PEC response.

Meanwhile, T. Higashi *et al.* introduced a fabrication method that merges sputtering with a solution-based process.[58] Initially, Ta_3N_5, the primary material, was deposited using a radiofrequency magnetron sputtering system. Subsequent surface modification involved applying electrocatalysts such as FeO_x, NiO_x, CoO_x, $NiFeO_x$, and $NiFeCoO_x$ to form metal-oxide catalysts, enhancing the PEC oxygen evolution reaction (OER) performance. Among these, the $NiFeO_x$-modified Ta_3N_5 ($NiFeO_x$/Ta_3N_5) photoanode showed the most promising onset potential for the OER. Consequently, a solar water-splitting cell with a parallel tandem configuration, incorporating the $NiFeO_x$/Ta_3N_5 photoanode and an Al-doped $La_5Ti_2Cu_{0.9}Ag_{0.1}S_5O_7$ (LTCA:Al) photocathode, was able to produce stoichiometric hydrogen and oxygen from water splitting without external bias, achieving a solar-to-hydrogen (STH) energy conversion efficiency of 0.2% within the first minute of reaction.

3.2. CVD process

CVD is pivotal for depositing thin films with customisable properties such as composition, thickness, and crystallinity, thereby optimising photoelectrode performance. It enables precise growth control, producing high-quality coatings or layers on the photoelectrode surface. CVD is versatile, allowing for the deposition of a wide range of complex materials and multilayered structures, paving the way for advanced photoelectrodes with enhanced functionalities.[59] The process employs chemical reactions to deposit materials from volatile precursors onto substrates, offering meticulous control over the composition and properties of the deposited layer or film. This precision facilitates the creation of complex materials and graded films designed for specific functionalities.[60]

The temperatures involved in CVD are typically higher than those in PVD, which allows for the deposition of a wider variety of materials and the growth of more complex films.[61] CVD systems are characterised by their complexity, requiring precise control over gas-phase reactions and often necessitating multiple precursor gases, leading to more elaborate setups and operational considerations.[62] CVD is particularly advantageous for applications that demand precise control over film composition and properties, such as semiconductor manufacturing, thin-film deposition, and surface engineering.[63] It is frequently

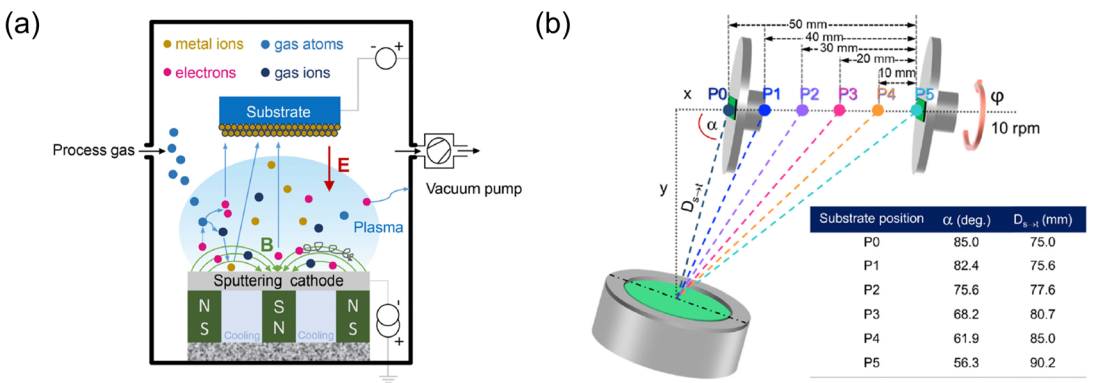

Fig. 3 (a) Schematic representation illustrating the principle of magnetron sputtering technology,[55] adapted with permission from ref. 55, copyright 2020 by Elsevier Ltd and Techna Group S.r.l. (b) Diagram of the magnetron sputtering with glancing angle deposition (MS-GLAD) technique,[56] indicating that the substrate can be adjusted from positions P0 to P5, adapted with permission from ref. 56, copyright 2021 by Elsevier Ltd and Techna Group S.r.l.

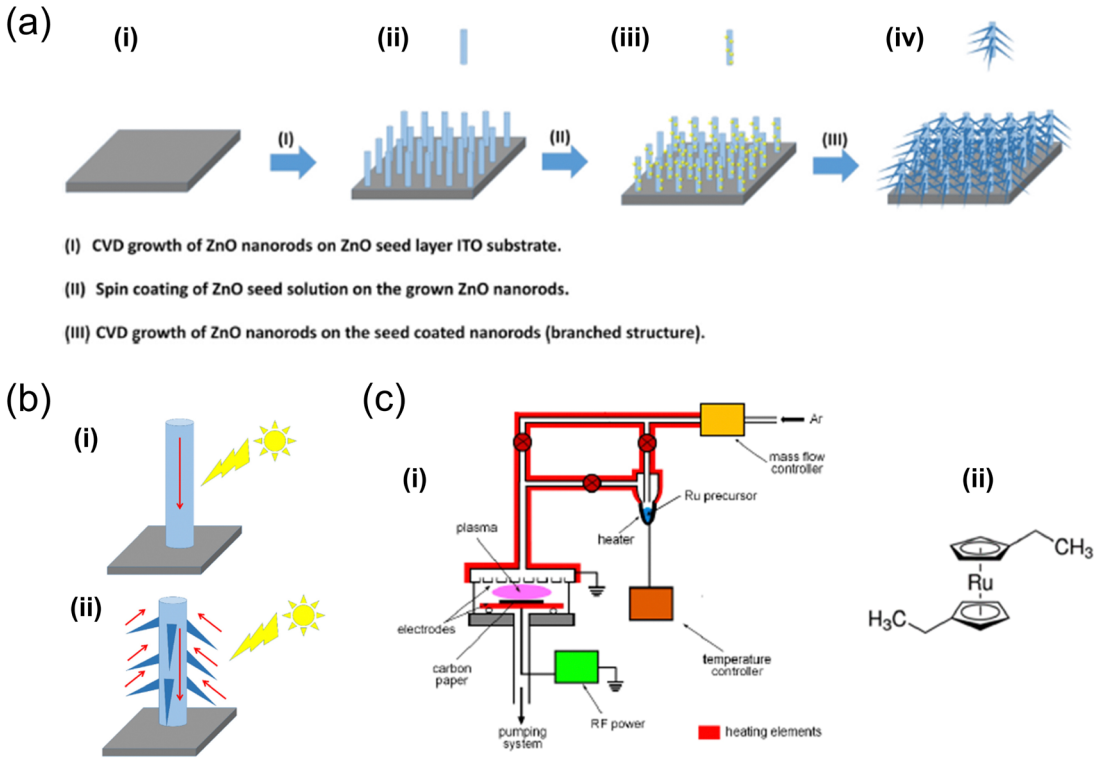

Fig. 4 (a) Illustration of the growth of both unbranched and branched ZnO nanorods using a CVD system.[64] (b) Comparison of photoresponses between (i) unbranched and (ii) branched ZnO nanorods. Reproduced with permission from ref. 64, copyright 2020 by Elsevier Ltd and Techna Group S.r.l. (c) Depicts (i) the RF plasma reactor utilised for the deposition of Ru-based films and (ii) the chemical structure of the Ru precursor.[67] Reproduced with permission from ref. 67, copyright 2020 by MDPI.

used to deposit protective coatings, passivation layers, or catalytic materials, thereby improving the stability, reactivity, and efficiency of solar water-splitting cells. Consequently, there are numerous solar water-splitting cells processed using CVD, with highly cited papers highlighted in this section (Fig. 4).

In 2021, S. A. Alharbi *et al.* developed several CVD-based solar water-splitting cells using both branched and unbranched ZnO nanorods.[64] The XRD analysis of the CVD-grown ZnO nanorods showed well-ordered, uniformly sized rods with a hexagonal-phase crystalline structure, exhibiting strong light-harvesting capabilities. The notable photoconversion efficiency of these ZnO nanorods indicates their potential in energy storage and conversion applications. Additionally, another study demonstrated the successful synthesis of bare and phosphorous-doped ZnO nanorods on fluorine-doped tin oxide (FTO)-coated glass *via* CVD. The integration of phosphorous and the hexagonal structure of the nanorods was verified using standard analytical techniques.[65] The results revealed that doping the ZnO nanorods with a small amount of phosphorous significantly improved their photoelectrochemical performance.

Furthermore, various researchers have investigated modifications to the CVD process. For example, K.C. Lau *et al.* utilised aerosol-assisted CVD (AACVD) to create solar water-splitting cells based on mixed iron–molybdenum multi-sulfide composite thin films. These films were deposited at 550 °C for 20 minutes using AACVD, with the concentration of the Cp_2Fe dopant varying (10, 20, 40, and 80 mol%).[66] PEC measurements showed that the thin film doped with 40 mol% Fe displayed the highest photocurrent density (1.241 mA cm^{-2}), whereas the 80 mol% Fe-doped film had a lower photocurrent density of 0.761 mA cm^{-2}, but exhibited the highest photosensitivity (1.396) due to the longest electron–hole recombination lifetime. Consequently, the amount and oxidation state of the doped iron significantly influenced the PEC performance of the molybdenum multi-sulfide composites.

Similarly, L. Jozwiak *et al.* utilised plasma-enhanced CVD (PECVD) to fabricate novel Ru-based thin catalytic films. X-ray photoelectron spectroscopy (XPS) analysis of the RuO_x thin films indicated that the as-deposited films were primarily composed of metallic Ru atoms (Ru^0) (primarily Ru^{4+} (RuO_2)), which transitioned to higher oxidation states after electrochemical stabilisation.[67] These stabilised films demonstrated exceptional catalytic OER activity, as shown by linear scanning voltammetry results at pH = 13.6, with onset potentials and 10 mV overpotentials of approximately 220 mV and 350 mV, respectively. Additionally, a photocurrent density of 9.0 mA cm^{-2} was obtained at 1.6 V (*vs.* RHE) in the photoelectrochemical process. Therefore, the plasma-deposited RuO_x catalysts emerged as potent alternatives for photoanode materials in solar water-splitting cells.

Y. Zhang *et al.* utilised dry-based CVD and solution-based processes to fabricate a heterojunction photoanode.[68]

Specifically, WO_3 and Fe_2O_3 composite heterojunction photoanodes were synthesised on an FTO substrate using hydrothermal and CVD methods, respectively. Compared to the pristine WO_3 nanostructure, the WO_3/Fe_2O_3 heterojunction photoanode exhibited a 1.25-fold increase in photocurrent density. The heterojunction formation accelerated the separation and migration of the photogenerated charge carriers and consequently inhibited their recombination. As a result, the PEC performance and stability of the heterojunction photoanode were improved under alkaline conditions.

3.3. ALD process

ALD systems utilise self-limiting surface reactions to deposit thin films with atomic-level precision. ALD offers atomic-level control over film thickness and composition, ensuring uniform and conformal coatings. This technique provides precise surface and interface engineering capabilities,[69,70] enabling the creation of conformal and pinhole-free coatings or layers that offer superior protection and passivation for photoelectrodes. ALD is particularly beneficial for depositing catalytic materials with a high surface area and uniform distribution, which promotes efficient water-splitting reactions and enhances overall PEC performance. Additionally, ALD operates at moderate-to-low temperatures, allowing for the deposition of thin films on a broad range of substrates, including those that are temperature-sensitive.[71] This feature is crucial for applications requiring atomic-level precision in thin-film deposition, such as semiconductor device fabrication, advanced coatings, and nanotechnology, where uniformity and precise film properties are paramount.[72] It enables the development of tailored surface properties, for example, controlled surface recombination, to minimise losses and enhance the efficiency of photoelectrodes in the water-splitting process. Therefore, ALD represents a transformative method (Fig. 5) that can supplant various chemical methods of CVD and physical methods of PVD for forming thin films in solar water-splitting cells.

ALD was utilised to deposit an ultrathin TiO_2 passivation layer on the main material in the study conducted by Y. Wang *et al.*, where the rGO/NiFe-LDH catalyst was applied to a Cu_2O photocathode.[73] A pristine Cu_2O nanostructure was electrodeposited onto an FTO substrate, followed by synthesising the decorated rGO/NiFe-LDH catalyst using hydrothermal methods. The ALD-deposited TiO_2 coating layer significantly mitigated photocorrosion and improved the chemical reaction kinetics of the Cu_2O photocathode. The current density reached -3.71 mA cm^{-2}, and the photoelectric conversion efficiency was 0.41%, underscoring the effectiveness of this method in enhancing Cu_2O applications in PEC water splitting.

In a related effort, A. Song *et al.* utilised an ALD system to create a passivation layer to prevent photocorrosion in a

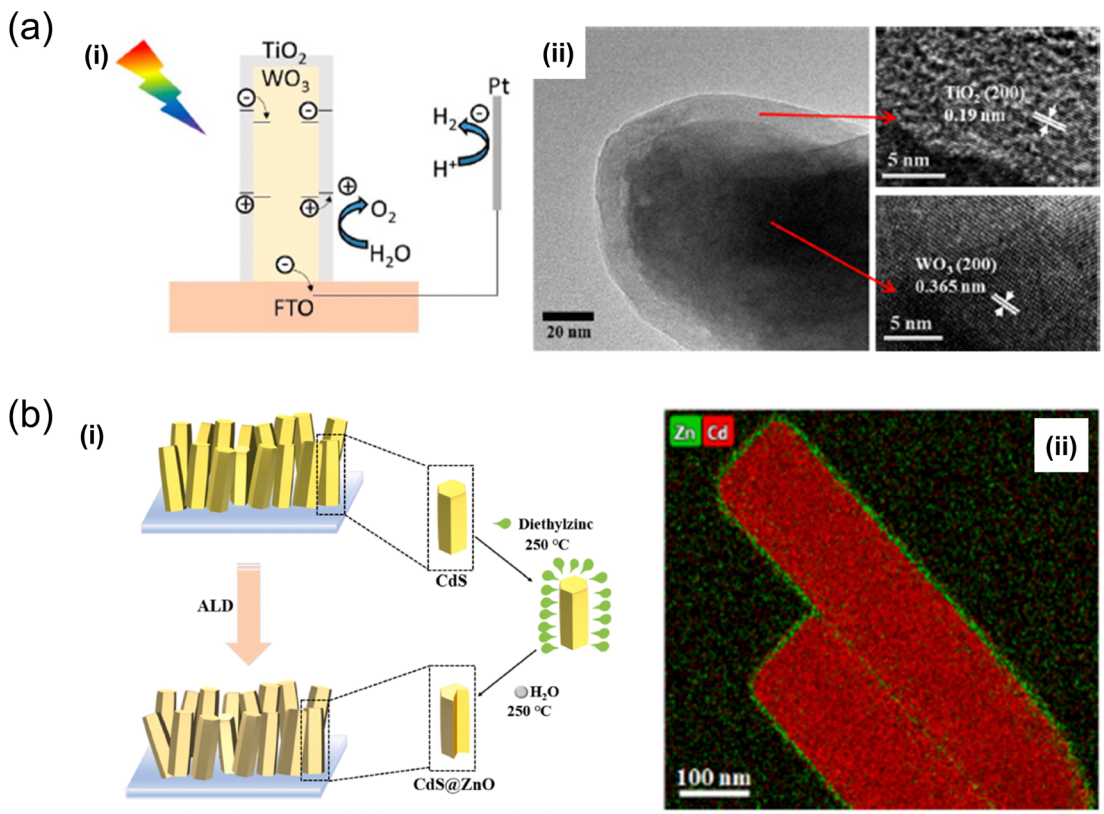

Fig. 5 (a) Schematic representation of charge transfer during (i) the photoelectrochemical reaction in WO_3/TiO_2 core–shell nanoplates, developed through hydrothermal treatment and ALD,[75] (ii) TEM images of TiO_2 layers formed after 200 ALD cycles on WO_3. Reproduced with permission from ref. 75, copyright 2020 by American Chemical Society. (b) Synthesis of (i) CdS@ZnO nanorod arrays *via* the ALD method[76] (ii) and the HAADFSTEM image of $CdS@ZnO_{200}$ core–shell nanorods of Zn and Cd. Reproduced with permission from ref. 76, copyright 2023 by Elsevier B.V.

W:$BiVO_4$–$CuBi_2O_4$ tandem solar water-splitting cell, employing a complex structure and various solution-based processes.[74] The W:$BiVO_4$ photoanode and $CuBi_2O_4$ photocathode were produced through spray pyrolysis. CoPi catalysts were electrodeposited on the W:$BiVO_4$ photoanode. For the photocathode, a CdS buffer layer and TiO_2 protection layer were established *via* chemical bath deposition and ALD, respectively. The RuO_x cocatalyst was photoelectrodeposited onto the $CuBi_2O_4$/CdS/TiO_2 structure. Despite the significant increase in the stability of the $CuBi_2O_4$ photocathode after the coating process, the photocurrent onset potential decreased, attributed to the CdS/TiO_2 heterojunction layer. Consequently, a tandem cell featuring W:$BiVO_4$/CoPi and $CuBi_2O_4$/CdS/TiO_2/RuO_x demonstrated hydrogen production under illumination with an applied bias of $\geq$0.4 V.

An ALD system was also utilised for precision coating and to develop a core–shell nanostructuring tool. For instance, using a hydrothermal method and ALD, K. Liu and T. Perng crafted a core–shell flower-like structured WO_3/TiO_2 nanoplate.[75] This core–shell structure exhibited enhanced PEC efficiency compared to pure WO_3 under AM 1.5 solar-light irradiation. Moreover, the hybrid structure could absorb substantial light and reduce the recombination rate of electron–hole pairs. In another study, X. Feng *et al.* reported improved hydrogen evolution efficiency with CdS@ZnO core–shell nanorod arrays developed through ALD in a solar water-splitting cell.[76] The CdS@ZnO core–shell nanorod arrays demonstrated a significantly higher H_2 evolution rate of 21.64 μmol h^{-1} cm^{-2}, nearly 9.4 times that of pristine CdS nanorod arrays. This improvement was attributed to the Z-scheme charge-transfer mechanism between the CdS core and ZnO shell, which facilitates the spatial separation of photoinduced electrons and holes and reduces the transfer resistance of charge carriers due to the close contact between the two semiconductors.

Additionally, the ALD process provided a doping effect on the main material in the study conducted by B. Alfakes *et al.* The researchers precisely introduced a hafnium (Hf) dopant into ZnO through ALD, enhancing its PEC performance.[77] Detailed analysis of the doped materials revealed a threefold increase in photocurrent for the best-performing sample (0.75-wt% Hf), attributed to the reduced surface recombination of photocarriers, thereby leading to more efficient PEC water oxidation. They concluded that ALD can be applied to introduce materials into the photoanode, combining unstable and highly active materials with an appropriate protective layer, potentially overcoming stability limitations.

ALD evidently contributes to enhancing the PEC performance of solar water-splitting cells. The findings from these studies underscore that ALD is an essential tool for designing and fabricating PEC electrodes for water splitting.

4. Laser-assisted fabrication processes for solar water-splitting cells

The laser processing of nanomaterials has garnered significant interest due to its precision in manipulating and modifying materials at the nanoscale.[78] This technique has found applications across various domains, including electronics,[79] bioelectronics,[80,81] energy,[82] and materials science.[83] The principal advantages of laser processing include its exceptional precision, which allows for the precise modification, cutting, and structuring of nanomaterials with minimal thermal impact on adjacent areas. It enables precise processing of nanoscale materials by focusing high energy density on localised areas. This allows for efficient material removal, annealing, or modification without affecting the entire material.[84] Additionally, laser processing is adaptable to a broad spectrum of nanomaterial shapes, such as nanoparticles, nanotubes, nanowires, and nanofilms, broadening its applicability in both academic and industrial settings.[84] Thus, laser processing significantly contributes to the advancement of nanoscale materials, enhancing their functionality and performance in emerging energy applications, including solar water-splitting cells.

This section explores various methods for fabricating solar water-splitting cells through laser-related processes, categorised into pulsed laser deposition (PLD), direct laser processing, laser-assisted synthesis, and other optical fabrication techniques. Although the discussion of PLD, typically conducted under vacuum conditions, slightly diverges from the primary focus of this review, which is to summarise advanced fabrication processes employing lasers without vacuum constraints, it is included for a comprehensive overview. Both vacuum and nonvacuum laser-related processes are discussed in this section. Detailed information on solar water-splitting cells fabricated using laser-based methods is compiled in Table 2.

4.1. PLD process

PLD is a physical thin-film deposition method that utilises intense laser pulses in a controlled vacuum to transfer materials from a target to a substrate. This process allows for precise control over the structural and compositional properties of the deposited films, making it possible to tailor materials for specific applications, such as solar water-splitting cells. The scalability and reproducibility of PLD (Fig. 6) show great potential for producing high-quality thin films for advanced energy conversion technologies.

M. Kölbach *et al.* prepared $BiVO_4$ thin films for solar water-splitting cells using PLD,[85] originating from a $BiVO_4$ target. The study systematically detailed PLD for $BiVO_4$ films, highlighting discrepancies from an ideal stoichiometric target-to-substrate material transfer. It explored the relationship between the V/Bi ratio of the films, their charge-carrier transport properties, and PEC performance, achieving AM 1.5 sulfite oxidation photocurrents of $\sim$2.4 mA cm^{-2} at 1.23 V (*vs.* RHE) without intentional doping or surface modification. Additionally, the creation of $BiVO_4$ photoelectrodes by alternating ablation of Bi_2O_3 and V_2O_5 targets was discussed as an innovative method to control cation stoichiometry, yielding $BiVO_4$ films with AM 1.5 sulfite oxidation photocurrents of up to 2.6 mA cm^{-2} at 1.23 V (*vs.* RHE). These findings provide crucial insights into the PLD of ternary oxide semiconductors, facilitating the accelerated synthesis and investigation of new metal-oxide photoelectrodes.

Table 2 Summarised data of the solar water-splitting cells fabricated by laser- and optical-based processes

Method	J_{max} (mA cm^{-2}) (at 1.23 V *vs.* RHE)	Material	Electrolyte	Ref.
PLD	2.60	$BiVO_4$	0.5 M KPi	85
PLD	5.70	Co_4O_4/pGO/$BiVO_4$/SnO_x–Pt/TiO_x/PIP/CuO_x	1.0 M KBi	86
PLD	0.91	TiO_2/Fe_2O_3	1 M KOH	87
LIPT[a]	1.146	Fe_2O_3	1 M NaOH	88
PLA[b]	0.484	Ti:Fe_2O_3	1 M NaOH	89
Laser treatment	4.43 (at 2.0 V *vs.* Ag/AgCl)	Cu–TiO_2	0.5 M Na_2SO_4 and 0.5 M KOH	90
LIPT	0.00843	TiO_2	1 M KOH	91
LIPR[c]	0.747	Fe_2O_3	1 M NaOH	92
LADC[d]	3.21	WO_3/FeNiOOH	0.5 M Na_2SO_4	93
Laser treatment	0.60	$BiVO_4$	0.1 M KPi	94
Laser treatment	0.908	TiO_2	1 M KOH	95
LICD[e]	3.16	WO_3/NC–FeOOH	0.5 M Na_2SO_4	96
PLIL[f]	1.45	Fe_2O_3@TiO_2–V_{Ti}	1 M KOH	97
LSPC[g]	2.28	Fe_2O_3/TiO_2–CdTe	1 M KOH	98
LSPC	6.22	LBSO:$BiVO_4$	1 M KPi	99
Laser treatment	6.08	Mo:$BiVO_4$	1 M KPi	100
Photoelectrodeposition	0.72 (at 1.5 V *vs.* RHE)	Pt–TiO_2	1 M KOH	101
Photoelectrodeposition	0.63	Fe_2O_3/NiOOH	1 M NaOH	102
Photoelectrodeposition	2.34	CoOOH/FeOOH/F—Fe_2O_3	1 M KOH	103
Photoelectrodeposition	4.30	$CoFeB_i$/$BiVO_4$	1 M K_3BO_3	104
Photoelectrodeposition	3.60	$Ni_2P_2O_7$–Nd–$BiVO_4$	0.5 M Na_2SO_4	105
Microwave-assisted synthesis	1.68 (at 1.0 V *vs.* Ag/AgCl)	WO_3 nanosheets	0.5 M Na_2SO_4	106
Microwave irradiation	1.37	Si/Ti:Fe_2O_3	1 M NaOH	107

[a] LIPT: laser induced phase transformation. [b] PLA: pulse laser annealing. [c] LIPR: laser-induced photoreduction. [d] LADC: laser-assisted defect control. [e] LICD: laser-induced catalyst deposition. [f] PILI: pulsed laser irradiation in liquid. [g] LSPC: laser synthesis and colloidal treatment.

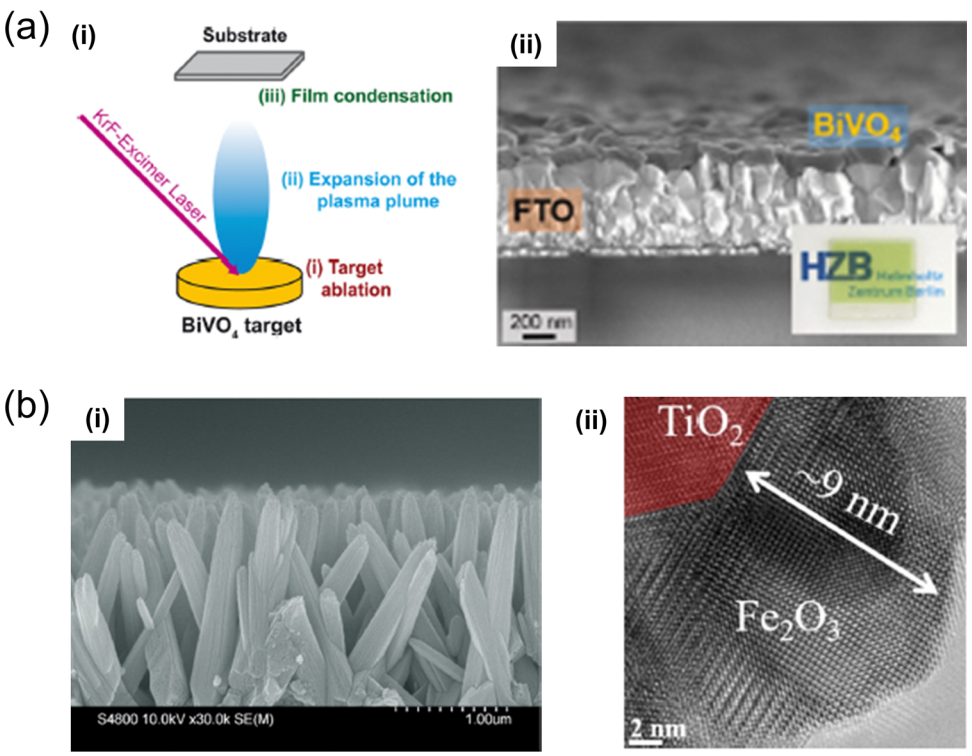

Fig. 6 (a) Illustration depicting (i) the trio of primary processes occurring in PLD using a $BiVO_4$ target.[85] (ii) SEM cross-sectional view of $BiVO_4$ films produced. Inset: An optical image of the FTO/$BiVO_4$ sample. Reproduced with permission from ref. 85, copyright 2020, American Chemical Society. (b) PLD-processed TiO_2/Fe_2O_3 core/shell nanostructure, engineered for enhanced stability and efficiency in visible-light-driven photoelectrochemical water splitting;[87] includes (i) a cross-sectional SEM representation, and (ii) a TEM visualisation. Reproduced with permission from ref. 87, copyright 2020 by American Chemical Society.

S. Ye *et al.* developed a $BiVO_4$-based photoanode for an overall unassisted PEC water-splitting system, integrating components like a Co_4O_4/pGO/$BiVO_4$/SnO_x photoanode and a Pt/TiO_x/PIP/CuO_x photocathode with multimediator modulation.[86] PLD was

used to form a $BiVO_4/SnO_x$ layer on the FTO electrode surface. The study revealed orderly electron transport from the $BiVO_4$ photoanode to an organic photocathode, driven by mediator potential differences, a reduced charge recombination rate, and an increased charge-transfer rate within the system. The strategic use of different mediators underscored their roles in enhancing charge transfer and minimising charge recombination. Moreover, combining a fully structured photoanode and photocathode yielded the highest charge-transfer efficiency compared to configurations without mediators. The employment of organic polymers enabled highly complementary light absorption between the organic photocathode and $BiVO_4$ photoanode, significantly boosting solar energy utilisation and leading to an impressive STH conversion efficiency of ~4.3%. These results underscore the critical importance of thoughtful design and assembly in creating effective dual-photoelectrode devices, particularly highlighting the benefits of complementary light absorption and efficient charge transfer.

Core–shell nanomaterials are pivotal in photoelectrochemistry, as they exhibit enhanced charge separation, improved light absorption, and tailored surface properties, offering versatile and scalable solutions for efficient energy conversion applications. PLD also contributes to synthesising core–shell nanostructures. H. Lu *et al.* successfully fabricated TiO_2/Fe_2O_3 core–shell heterojunction nanorod arrays using PLD, which was then applied as a photoelectrode in efficient solar water-splitting cells.[87] The study extensively analysed the morphology, phase, and carrier transfer mechanisms of both pristine TiO_2 and TiO_2/Fe_2O_3 core–shell nanostructures. PEC measurements indicated that the photocurrent density of the TiO_2/Fe_2O_3 core–shell nanostructure nearly doubled compared to that of the pristine TiO_2 structures. Additionally, visible-light absorption expanded from 400 to 550 nm, the charge separation rate was enhanced, and exceptional stability was demonstrated, with only a 3% decrease in current density after 14 days of testing. This research illustrates a method for designing efficient nanostructures through a combination of a simple hydrothermal process and a high-quality PLD process with significant potential for versatile expandability.

4.2. Direct laser process

The direct laser process, a prevalent method in material processing, employs lasers to directly impact target materials, inducing photothermal, photochemical, and photothermochemical effects. These effects include sintering, ablation, annealing, and reduction of materials. This method minimises material waste and enables a high degree of customisation. It is particularly effective for the rapid phase change and fabrication of complex structures. The direct laser process (Fig. 7) stands out as an advanced and alternative fabrication technique, promising as a tool for developing advanced photoelectrodes for solar water-splitting cells and other renewable energy applications.

Exploring the photothermal effect of laser processing offers an innovative approach to manipulating metal oxides. J. Yeo's research group demonstrated this by fabricating metal-oxide-based solar water-splitting cells with enhanced PEC performance. Specifically, they employed laser processing as a novel post-annealing technique to improve the PEC performance of hematite nanorod photoanodes.[88] The focused laser beam created a highly localised high-temperature field, facilitating the transformation of akaganeite (β-FeOOH) into hematite (α-Fe_2O_3) and the diffusion of Sn from the FTO glass. This laser-induced phase transformation (LIPT) process resulted in exceptional water oxidation performance without damaging the FTO glass substrates, thanks to its precise localisation and instantaneous action. The hematite photoanodes produced through the LIPT process showed significantly enhanced electrical resistance, crystallinity, and optical absorbance, culminating in superior PEC performance.

Similarly, D. Wang *et al.* introduced a pulse laser annealing (PLA) strategy to activate titanium dopants on hematite photoanodes, aiming for improved PEC performance.[89] High-temperature annealing, a common method for activating dopants on metal oxides, often results in considerable thermal damage to the conductive substrate. The laser annealing technique circumvents this issue, activating dopants while

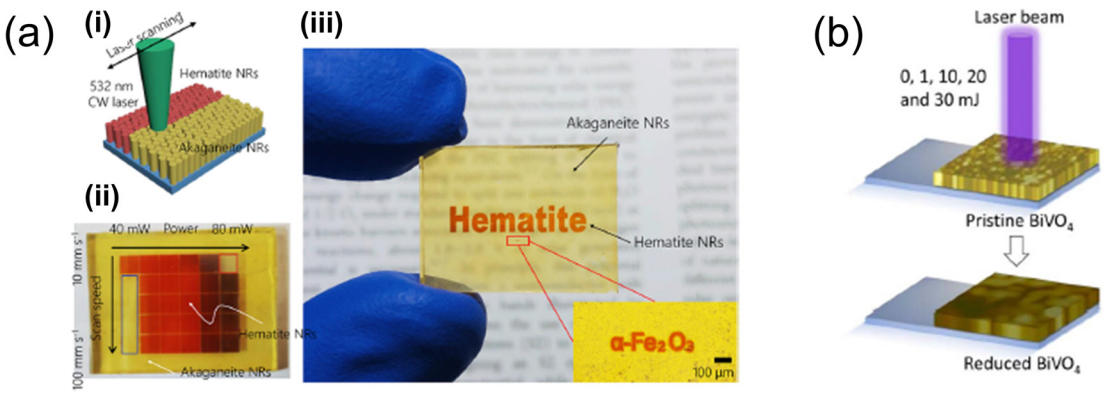

Fig. 7 (a) Illustration depicting (i) the laser-induced selective phase transformation process applied to hematite nanorods (NRs);[88] (ii) combinatorial study of optimal laser power with laser scanning speed for akaganeite NRs on FTO glass substrates; (iii) laser-patterned hematite NRs displaying letters created with the laser scanner. Reproduced with permission from ref. 88, copyright 2020 by American Chemical Society. (b) Schematic showing the laser-based reduction method used for $BiVO_4$ photoanodes.[94] Reproduced with permission from ref. 94, copyright 2022 by American Chemical Society.

minimising thermal damage effectively. The Ti:Fe_2O_3 photoanode treated with laser exhibited improved crystallinity compared to its untreated counterpart, doubling the photocurrent density. Additionally, the surface charge transfer efficiency more than doubled, and the donor density increased significantly, from 1.28×10^{18} cm^{-3} to 1.29×10^{19} cm^{-3}. These findings underscore the potential of PLA treatment in enhancing dopant activation and, consequently, the performance of photoanodes for PEC applications.

K. G *et al.* proposed a method for annealing thin copper-coated TiO_2 nanotubes using a laser process to enhance PEC performance.[90] This fast and straightforward method enables selective modification of the nanostructures' surface to achieve desired shapes and sizes. The samples prepared by this laser method (L60-Cu–TiO_2 and L120-Cu–TiO_2) showed increased absorbance in the visible light spectrum compared to pure TiO_2, with the current density observed to improve by approximately sevenfold under both dark and illuminated conditions. This enhancement is ascribable to the synergistic effects of laser-induced morphological and optical property changes, making this approach viable for producing TiO_2 nanotubes with outstanding electrochemical activity for the OER.

M. Qiao *et al.* introduced an innovative approach to transform the phase of TiO_2 nanotubes using femtosecond laser processing.[91] This method selectively alters the crystal facet phase of the anatase samples, boosting the photocurrent density by more than five times compared to the unaltered anatase TiO_2 nanotube photoanode, from 1.59 μA cm^{-2} to 8.43 μA cm^{-2}. Additionally, the photoluminescence intensity of the TiO_2 nanotubes prepared by laser processing was lower than that of the pristine anatase TiO_2 nanotube photoanode, indicating improved charge separation efficiency for photogenerated carriers. Thus, the proposed laser annealing processing strategy holds promise not only for PEC applications but also for the development of functional nanomaterials.

In a separate study, J. Yeo's research group investigated the interaction between the laser's photothermal and photothermochemical effects on hematite nanorods. They explored laser-induced photoreduction (LIPR) of hematite nanorods with dual objectives: to create patterned arrays of magnetite nanorods and to enhance the performance of hematite nanorods in PEC water oxidation by engineering oxygen vacancies (OVs).[92] A CW laser beam with a wavelength of 532 nm was directed at hematite nanorods immersed in an ethylene glycol (EG) solution, providing the thermal energy necessary for the Fe^{3+} reduction reaction. They successfully converted hematite nanorods into magnetite using adequate laser power during the LIPR process. OV-rich hematite nanorods were produced at lower laser powers, serving as an intermediary stage before transforming into magnetite. These OV-rich hematite nanorods showed significantly improved donor density and electrical conductivity, attributed to OVs acting as additional electron donors, leading to enhanced PEC water oxidation performance.

Expanding on OV engineering to manipulate the lattice defects of metal oxides, H. Kong *et al.* reported utilising the laser-assisted defect control (LADC) process on monoclinic tungsten trioxide (m-WO_3) to enhance PEC performance.[93] The study particularly focused on the correlation between the spatial distribution of OV defects in m-WO_3 photoanodes and their PEC performance. It was confirmed that a higher concentration of OVs near the surface of m-WO_3, compared to its bulk, was beneficial for PEC performance. Consequently, LADC enabled precise manipulation of the spatial distribution of OVs on the m-WO_3 photoanode surface, leading to improved PEC performance.

Similarly, M. Barawi *et al.* applied laser irradiation to improve the water oxidation properties of $BiVO_4$ photoanodes through surface reduction.[94] This technique selectively reduced surface-level V atoms, inducing OV formation without altering the film's bulk structure. The modifications were confirmed by XPS and X-ray absorption spectral analyses. The resulting samples exhibited effective n-doping, marked by a shift in the VB maximum to higher binding energy, which enhanced charge transport and created a more favourable VB position for water oxidation. Additionally, the treated samples showed an extended lifetime for photogenerated holes, reduced charge-transfer resistance, and an accumulation of holes at the surface, collectively reducing recombination and boosting charge extraction. These effects collectively doubled the photocurrent density of the laser-treated samples compared to the untreated ones.

Furthermore, T. Nakajima *et al.* explored the generation of OVs in TiO_2 films[95] using laser irradiation, which led to improved PEC performance over pristine TiO_2 films. The STH efficiency of the treated TiO_2 was 0.52%, approximately 2.6 times higher than that of the untreated TiO_2 film. This enhancement was attributed to oxygen deficiency, which increased the density of electron donors in the photoanode, improving charge transport and overall PEC performance. Additionally, laser irradiation altered the cross-sectional morphology of the TiO_2 film, increasing the carrier diffusion length and further boosting the PEC properties of the photoanode.

4.3. Laser-assisted synthesis

Laser-assisted synthesis methods (Fig. 8) utilise a laser to deposit or synthesise catalytic materials and protective coating layers on photoelectrode surfaces. This technique offers high precision and control, enabling the creation of well-defined catalytic structures and protective layers, which enhance catalytic efficiency and prevent photocorrosion in solar water-splitting reactions.

H. Kim *et al.* employed laser-induced catalyst deposition (LICD) to deposit FeOOH and Ni- and Co-doped FeOOH cocatalysts onto WO_3 photoanodes.[96] By adjusting the elemental composition and combining Ni, Co, and Fe in the liquid precursor, Ni- and Co-doped FeOOH cocatalysts were effectively formed with a thickness of approximately 5 nm on the WO_3 photoanodes *via* LICD. The WO_3 photoanode featuring Ni- and Co-doped FeOOH cocatalysts demonstrated a photocurrent exceeding 3 mA cm^{-2} at 1.23 V (*vs.* RHE). The lifespan of photoexcited carriers was analysed through time-resolved photoluminescence, measuring luminescence signals from carrier recombination. Distinguishing luminescent photons

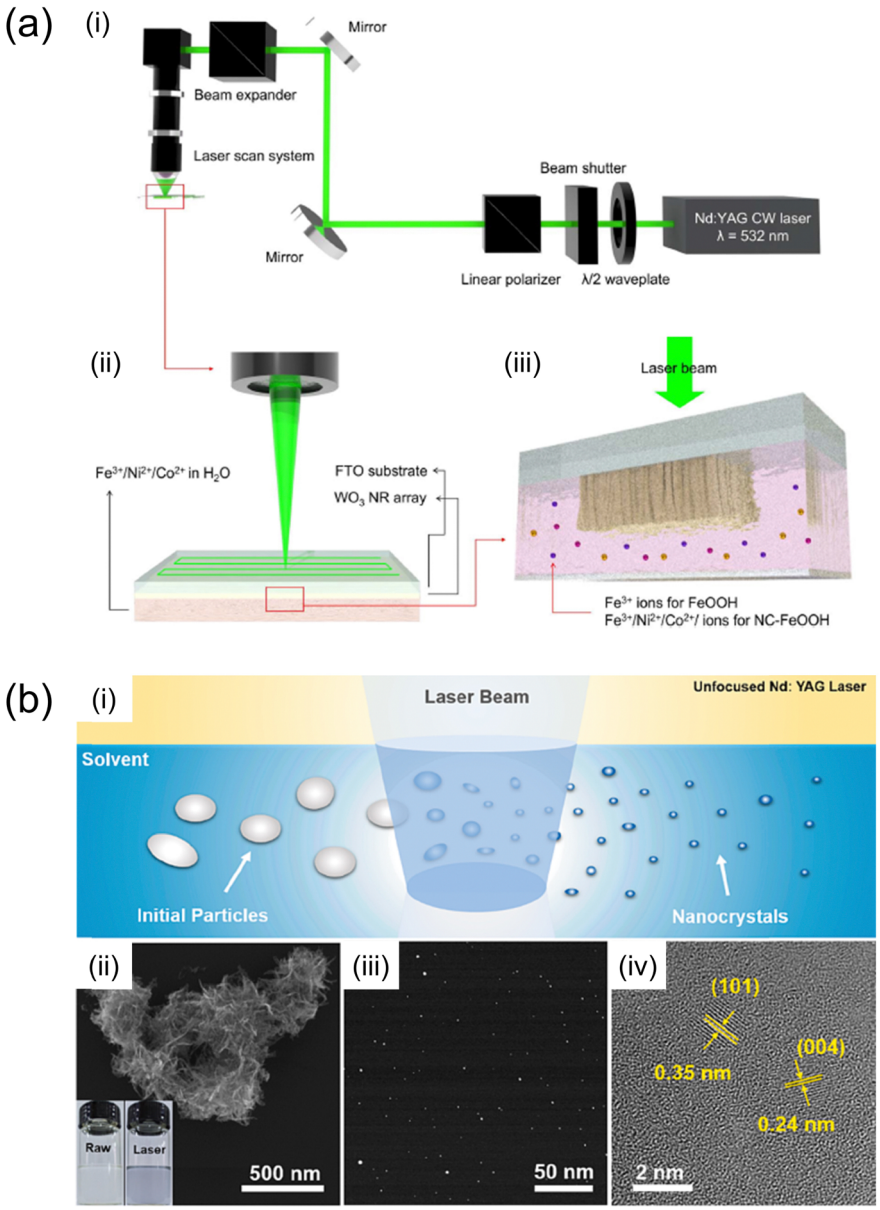

Fig. 8 (a) Schematic diagram of (i) an optical system for LICD. (ii) Schematic diagram of LICD reaction. A CW laser beam with a wavelength of 532 nm was employed to scan the entire sample area. (iii) WO_3 NRs are immersed in an aqueous solution containing Ni^{2+}, Co^{2+} and Fe^{3+} ions.[96] Reproduced with permission from ref. 96, copyright 2023 by The Royal Society of Chemistry. (b) TiO_2–V_{Ti} before and after PLIL.[97] (i) Schematic illustration of the preparation of TiO_2–V_{Ti} nanocrystals *via* PLIL. (ii) SEM image of TiO_2–V_{Ti} raw materials before PLIL (inset: the optical image of TiO_2–V_{Ti} raw materials dispersed in ethanol before (left) and after PLIL (right)). (iii) STEM image of the TiO_2–V_{Ti} nanocrystals and (iv) their HRTEM image. Reproduced with permission from ref. 97, copyright 2023 by Elsevier B.V.

with $\lambda < 500$ nm and those with $\lambda > 500$ nm using short-pass and long-pass optical filters, respectively, it was found that the Ni- and Co-doped FeOOH cocatalysts significantly prolonged the lifetime of photoexcited holes with $\lambda > 500$ nm. This suggests that trap-mediated recombination was inhibited, with the cocatalysts providing hole-storing trap states that extend the lifespan of trapped holes, thereby enhancing water oxidation photocurrents.

Similarly, H. Kong *et al.* conducted a one-step laser deposition process to deposit an FeNiOOH catalyst overlayer on monoclinic m-WO_3 nanorods (NRs).[93] An FeNiOOH layer ~2 nm thick was successfully deposited on the WO_3 NR. The FeNiOOH-catalyst-deposited monoclinic m-WO_3 sample exhibited an increase in photocurrent from 2.13 mA cm^{-2} to 3.21 mA cm^{-2} at 1.23 V (*vs.* RHE), which marks an improvement of approximately 51% over the pristine monoclinic m-WO_3 sample. Furthermore, the FeNiOOH catalyst-deposited monoclinic m-WO_3 sample displayed a negative shift in the dark current onset potential and enhanced stability.

Meanwhile, F. Li *et al.* executed nanocrystal synthesis in a liquid precursor *via* the pulsed laser irradiation in liquid (PLIL) technique.[97] To bolster the PEC performance of Fe_2O_3

photoanodes, the PLIL process was utilised to incorporate sub-5-nm p-type Ti-defected TiO_2 nanocrystals into a Fe_2O_3 matrix. This approach significantly boosted the photocurrent density from 0.27 to 1.45 mA cm^{-2} at 1.23 V (*vs.* RHE) and reduced the carrier transport time from 159 to 38 μs. The nano-heterostructures produced through the PLIL process not only expedited the separation of photogenerated electron–hole pairs but also enhanced carrier transport, leading to improved PEC performance.

To enhance the charge transfer efficiency of metal oxides, H. Wang and colleagues applied laser synthesis and colloidal treatment (LSPC) strategies.[98] They developed embedded p–n heterojunctions within a hematite photoanode using the LSPC process. Subsequently, introducing a passivation layer (TiO_2–CdTe) onto the hematite resulted in a substantial improvement in PEC performance. This enhancement was evidenced by a 12-fold increase in the lifetime of photogenerated carriers, a 3.9-fold increase in the injection efficiency η_{inj} at 1.23 V (*vs.* RHE), and an increase in the photocurrent density at 1.23 V (*vs.* RHE) by 4.4 times. Furthermore, the LSPC process was employed to incorporate laser-generated nanocrystals (LBSO) into the $BiVO_4$ photoanode,[99] achieving a photocurrent density increase from 4.01 mA cm^{-2} to 5.15 mA cm^{-2} at 1.23 V (*vs.* RHE) for a single $BiVO_4$ photoanode configuration and 6.22 mA cm^{-2} at 1.23 V (*vs.* RHE) for a dual configuration. The LBSO:$BiVO_4$ photoanode, prepared *via* LSPC, exhibited enhanced charge transfer efficiency alongside increased carrier mobility and lifetime. This research offers an innovative approach to overcoming poor charge transport and augmenting PEC performance.

To mitigate photocorrosion in water splitting, J. Jian and associates introduced advanced techniques for creating a stable and active semiconductor–liquid junction (SCLJ).[100] They innovated a dual interfacial layer structure on Mo:$BiVO_4$ (MBVO) photoanodes using laser-generated carbon dots with phenolic hydroxyl groups (LGCDs–PHGs), which protected against photocorrosion and augmented charge separation and transfer, thereby facilitating highly efficient and stable PEC activity. The enhancement in PEC activity was attributed to the improved charge density of the shallow MBVO-OV layer and the effective charge extraction and band alignment facilitated by the LGCD–PHG layer. The uniform application of this dual interfacial layer not only improved interfacial charge-carrier kinetics but also mitigated photocorrosion, leading to increased operational stability. Notably, the FeNiOOH–LGCD-PHG–MBVO photoanode, in a dual configuration, showcased a significant photocurrent density of up to 6.08 mA cm^{-2} at 1.23 V (*vs.* RHE) and maintained operational stability over 120 h. The proposed methodology, leveraging laser–matter interaction, proved generally advantageous for employing catecholic molecules to develop an effective SCLJ with enhanced PEC performance.

5. Other optical fabrication processes for solar water-splitting cells

In this section, we discuss optical fabrication processes, including a high-powered lamp system and microwave-assisted synthesis (Fig. 9). The high-powered lamp system enables the synthesis of cocatalysts over a large area through a straightforward method. T. Sharifi *et al.* developed self-ordered chromium-doped TiO_2 nanotubes (CT) using electroanodization, followed by cocatalyst deposition of Pt and Pd particles *via* photodeposition facilitated by the high-powered lamp.[101] The CT structures were uniform in size and shape, featuring an even distribution of Pt and Pd on the surface. However, the formation of noble metal clusters was influenced by the duration of the photodeposition process. Analytical results revealed that the Pt–CT and Pd–CT electrodes exhibited improved photogenerated electron–hole separation and transport properties, leading to significantly enhanced photocurrent responses compared to pristine CT electrodes. Additionally, H_2 generation tests showed that the hydrogen production rates for the Pt–CT and Pd–CT electrodes (1.08 and 0.65 mL cm^{-2} h^{-1}, respectively) were greater than that of the CT electrode (0.26 mL cm^{-2} h^{-1}).

Similarly, Y. Chen's research group introduced a photo-assisted electrodeposition method for efficiently fabricating photoanodes on α-Fe_2O_3.[102] This approach enabled the successful deposition of cocatalysts onto Fe_2O_3 photoanodes. As a result, the photocurrent density of the α-Fe_2O_3/NiOOH photoanode prepared by the photoassisted electrodeposition method (α-Fe_2O_3/NiOOH-ph) reached 626.137 μA cm^{-2} at 1.23 V (*vs.* RHE), which is approximately four times that of the pristine α-Fe_2O_3 photoanode and double that of the α-Fe_2O_3/NiOOH photoanode prepared by conventional electrodeposition. Additionally, the α-Fe_2O_3/NiOOH-ph photoanode exhibited reduced photogenerated carrier charge transfer resistance at the interface and a lower onset potential, enhancing charge transfer efficiency compared to the pristine α-Fe_2O_3 photoanode.

Furthermore, the research groups of G. Hu, Wang, and Jin employed a similar method of metal hydroxide catalyst deposition on the photoanode through photo-assisted electrodeposition. Hu's group demonstrated a strategy that not only improved the sluggish OER kinetics but also enhanced the PEC performance of the photoanode. The CoOOH/FeOOH/F-Fe_2O_3 photoanode achieved a current density of 2.34 mA cm^{-2} at 1.23 V (*vs.* RHE), which is 3.3 times higher than that of the pristine α-Fe_2O_3 photoanode.[103] Wang's group observed an increase in photocurrent for the $BiVO_4$ photoanode, approximately 2.6 times higher than that of the pristine $BiVO_4$,[104] along with improved PEC performance, including decreased carrier recombination and increased applied bias photon-to-current and incident-photon-to-electron conversion efficiencies. Jin's group found that the introduction of the $Ni_2P_2O_7$ cocatalyst accelerated the water oxidation reaction and enhanced the PEC performance of $BiVO_4$.[105] The $Ni_2P_2O_7$–Nd–$BiVO_4$ (3.6 mA cm^{-2}) photoanode prepared by photoassisted electrodeposition exhibited a higher photocurrent density (3.6 mA cm^{-2}) compared to the bare $BiVO_4$ photoanode (1.2 mA cm^{-2}).

M. A. Mahadik *et al.* explored the PEC performance and the growth mechanism of WO_3 nanosheet (NS) photoanodes on tungsten foils using microwave-assisted (MW-assisted) synthesis.[106] The growth of the WO_3–NS photoanodes was achieved

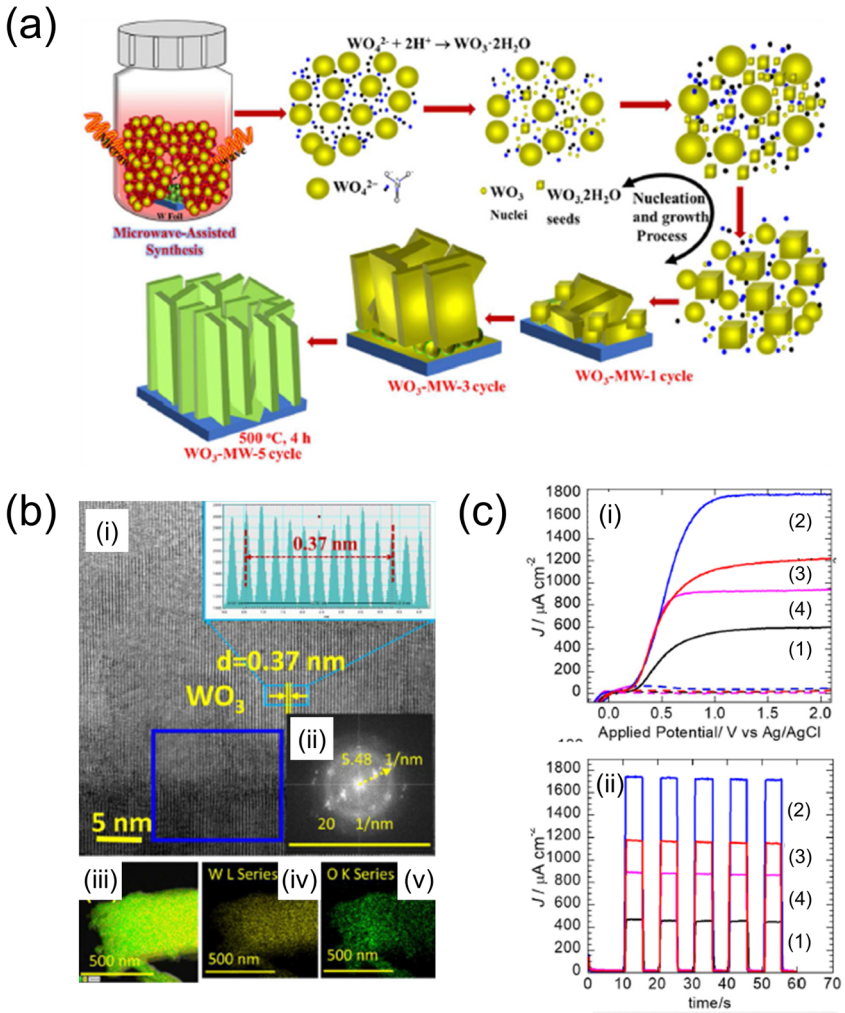

Fig. 9 (a) Schematic of the experimental steps for the microwave-assisted synthesis of WO_3 nanosheets on the W foil.[106] (b) HR-TEM images of the area highlighted in (i), with the corresponding lattice fringe distribution depicted in the inset. (ii) Fast Fourier transform (FFT) patterns corresponding to the highlighted blue square in (i). (iii)–(v) EDX elemental mapping of microwave-assisted optimum WO_3-MW-3 cycle. (c) (i) J–V and (ii) J–t curves of (1) WO_3-MW-1, (2) WO_3-MW-3 and (3) WO_3-MW-5 cycles, and (4) WO_3-MW-3 cycle-non-polished photoanodes annealed at 500 °C, 4 h, respectively. Reproduced with permission from ref. 106, copyright 2022 by Elsevier B.V.

through varying numbers of deposition cycles (one, three, and five times) with a constant microwave synthesis duration of 30 min. The photoanode deposited through three cycles exhibited the highest photocurrent density, reaching 1.68 mA cm^{-2} at 1.0 V (*vs* Ag/AgCl). The WO_3–NS photoanode, also deposited in three cycles, demonstrated efficient H_2 and O_2 evolution and significant degradation of the PEC orange II dye within 3 h, indicating its potential for diverse applications such as photovoltaics and electrocatalysis.

Similarly, T. Koh *et al.* demonstrated an MW-assisted synthesis technique for fabricating an Si and Fe_2O_3 photoanode (Si/Ti:Fe_2O_3).[107] They addressed high charge recombination and charge transfer kinetics by forming a homojunction. The thickness of the Si/Ti:Fe_2O_3 photoanode was adjusted by altering the MW irradiation time. The optimised homojunction (Si/Ti:Fe_2O_3) photoanode achieved a photocurrent density of 1.37 mA cm^{-2} at 1.23 V (*vs.* RHE) and exhibited an onset potential shift compared to the bare Ti–Fe_2O_3 photoanode, significantly enhancing charge separation and carrier transfer. This research suggests a cost-effective method for fabricating homojunction photoanodes using microwave-assisted synthesis. Comprehensive data for various solar water-splitting cells fabricated by other optical-based processes are summarised in Table 2.

6. Challenges and outlooks

This review highlights the potential of laser-assisted and other optical fabrication processes as alternatives to conventional vacuum-based methods for manufacturing solar water-splitting cells. Laser-assisted fabrication aims to reduce manufacturing costs by using cost-effective materials and nonvacuum deposition techniques, thereby improving the economic viability of solar water-splitting cell production. Additionally, scalability is a notable advantage of laser-assisted and other

optical-based methods. Employing high-speed laser scanning systems and high-powered lamp facilities can cover larger surface areas, making these methods suitable for mass production and commercial applications.

The potential of laser-assisted fabrication processes is poised to revolutionise the field through significant advancements in materials science and manufacturing technologies. The exploration of new materials, coupled with the advent of sophisticated laser techniques, is anticipated to substantially enhance the efficiency of solar water-splitting cells. These innovations are not only expected to improve performance through better light absorption and charge separation but also to provide an avenue for integrating these systems with renewable energy sources, thereby moving towards a more sustainable and decentralised energy infrastructure.

In summary, laser-assisted fabrication processes, typically low-temperature and non-vacuum-based, offer several advantages over conventional vacuum-based methods. These advantages include the flexibility in material selection and the feasibility of solution processes, particularly for the deposition of cocatalysts. As technology progresses and researchers devise innovative solutions, laser-based processes may emerge as competitive alternatives for fabricating solar water-splitting cells, promising greater efficiency and scalability. However, ongoing research and development efforts are essential to fully realise their potential in this domain.

Author contributions

J. Kwon: conceptualization, investigation, data curation, visualization, writing – original draft; S. Ko: data curation, investigation, writing – original draft; H. Kim: investigation, visualization; H. J. Park: data curation; C. Lee: investigation; and J. Yeo: conceptualization, supervision, writing – reviewing and editing.

Conflicts of interest

The authors declare no conflict of interest.

Acknowledgements

This research was supported through the Industrial Technology Innovation Program (no. 20023014) funded by the Ministry of Trade, Industry & Energy (MOTIE, Korea) and a National Research Foundation of Korea (NRF) grant funded by the Korean government (NRF-2018R1A6A1A06024970 and NRF-2022R1F1A1074802). This work was also supported by the Commercialization Promotion Agency for R&D Outcomes (COMPA) grant funded by the Korean Government (Ministry of Science and ICT) (RS-2023-00304695).

References

1 R. E. Neale, P. W. Barnes, T. M. Robson, P. J. Neale, C. E. Williamson, R. G. Zepp, S. R. Wilson, S. Madronich, A. L. Andrady, A. M. Heikkilä, G. H. Bernhard, A. F. Bais, P. J. Aucamp, A. T. Banaszak, J. F. Bornman, L. S. Bruckman, S. N. Byrne, B. Foereid, D. P. Häder, L. M. Hollestein, W. C. Hou, S. Hylander, M. A. K. Jansen, A. R. Klekociuk, J. B. Liley, J. Longstreth, R. M. Lucas, J. Martinez-Abaigar, K. McNeill, C. M. Olsen, K. K. Pandey, L. E. Rhodes, S. A. Robinson, K. C. Rose, T. Schikowski, K. R. Solomon, B. Sulzberger, J. E. Ukpebor, Q. W. Wang, S. Å. Wängberg, C. C. White, S. Yazar, A. R. Young, P. J. Young, L. Zhu and M. Zhu, Environmental effects of stratospheric ozone depletion, UV radiation, and interactions with climate change: UNEP Environmental Effects Assessment Panel, Update 2020, *Photochem. Photobiol. Sci.*, 2021, **20**, 1–67.

2 V. Radchuk, T. Reed, C. Teplitsky, M. van de Pol, A. Charmantier, C. Hassall, P. Adamík, F. Adriaensen, M. P. Ahola, P. Arcese, J. Miguel Avilés, J. Balbontin, K. S. Berg, A. Borras, S. Burthe, J. Clobert, N. Dehnhard, F. de Lope, A. A. Dhondt, N. J. Dingemanse, H. Doi, T. Eeva, J. Fickel, I. Filella, F. Fossøy, A. E. Goodenough, S. J. G. Hall, B. Hansson, M. Harris, D. Hasselquist, T. Hickler, J. Joshi, H. Kharouba, J. G. Martínez, J.-B. Mihoub, J. A. Mills, M. Molina-Morales, A. Moksnes, A. Ozgul, D. Parejo, P. Pilard, M. Poisbleau, F. Rousset, M.-O. Rödel, D. Scott, J. C. Senar, C. Stefanescu, B. G. Stokke, T. Kusano, M. Tarka, C. E. Tarwater, K. Thonicke, J. Thorley, A. Wilting, P. Tryjanowski, J. Merilä, B. C. Sheldon, A. Pape Møller, E. Matthysen, F. Janzen, F. S. Dobson, M. E. Visser, S. R. Beissinger, A. Courtiol and S. Kramer-Schadt, Adaptive responses of animals to climate change are most likely insufficient, *Nat. Commun.*, 2019, **10**, 3109.

3 K. E. Trenberth, Climate change caused by human activities is happening and it already has major consequences, *J. Energy Nat. Resour. Law*, 2018, **36**, 463–481.

4 S. Brönnimann, in *The Palgrave Handbook of Climate History*, ed. S. White, C. Pfister and F. Mauelshagen, Palgrave Macmillan, UK, London, 2018, pp. 321–328.

5 T. M. Letcher, in *Climate Change*, ed. T. M. Letcher, Elsevier, 3rd edn, 2021, pp. 3–17.

6 R. Chai, J. Mao, H. Chen, Y. Wang, X. Shi, M. Jin, T. Zhao, F. M. Hoffman, D. M. Ricciuto and S. D. Wullschleger, Human-caused long-term changes in global aridity, *npj Clim. Atmos. Sci.*, 2021, **4**, 65.

7 K. O. Yoro and M. O. Daramola, in *Advances in Carbon Capture*, ed. M. R. Rahimpour, M. Farsi and M. A. Makarem, Woodhead Publishing, 2020, pp. 3–28.

8 W. F. Lamb, T. Wiedmann, J. Pongratz, R. Andrew, M. Crippa, J. G. J. Olivier, D. Wiedenhofer, G. Mattioli, A. A. Khourdajie, J. House, S. Pachauri, M. Figueroa, Y. Saheb, R. Slade, K. Hubacek, L. Sun, S. K. Ribeiro, S. Khennas, S. de la Rue du Can, L. Chapungu, S. J. Davis, I. Bashmakov, H. Dai, S. Dhakal, X. Tan, Y. Geng, B. Gu and J. Minx, A review of trends and drivers of greenhouse gas emissions by sector from 1990 to 2018, *Environ. Res. Lett.*, 2021, **16**, 073005.

9 L. Warszawski, E. Kriegler, T. M. Lenton, O. Gaffney, D. Jacob, D. Klingenfeld, R. Koide, M. M. Costa, D. Messner,

N. Nakicenovic, H. J. Schellnhuber, P. Schlosser, K. Takeuchi, S. Van Der Leeuw, G. Whiteman and J. Rockström, All options, not silver bullets, needed to limit global warming to 1.5 °C: a scenario appraisal, *Environ. Res. Lett.*, 2021, **16**, 064037.

10 J. O. Abe, A. P. I. Popoola, E. Ajenifuja and O. M. Popoola, Hydrogen energy, economy and storage: Review and recommendation, *Int. J. Hydrogen Energy*, 2019, **44**, 15072–15086.

11 S. Dutta, A review on production, storage of hydrogen and its utilization as an energy resource, *J. Ind. Eng. Chem.*, 2014, **20**, 1148–1156.

12 F. Dawood, M. Anda and G. M. Shafiullah, Hydrogen production for energy: An overview, *Int. J. Hydrogen Energy*, 2020, **45**, 3847–3869.

13 Z. Abdin, A. Zafaranloo, A. Rafiee, W. Mérida, W. Lipiński and K. R. Khalilpour, Hydrogen as an energy vector, *Renewable Sustainable Energy Rev.*, 2020, **120**, 109620.

14 S. Sharma and S. K. Ghoshal, Hydrogen the future transportation fuel: From production to applications, *Renewable Sustainable Energy Rev.*, 2015, **43**, 1151–1158.

15 M. Hermesmann and T. E. Müller, Green, Turquoise, Blue, or Grey? Environmentally friendly Hydrogen Production in Transforming Energy Systems, *Prog. Energy Combust. Sci.*, 2022, **90**, 100996.

16 A. Ajanovic, M. Sayer and R. Haas, The economics and the environmental benignity of different colors of hydrogen, *Int. J. Hydrogen Energy*, 2022, **47**, 24136–24154.

17 S. Shiva Kumar and H. Lim, An overview of water electrolysis technologies for green hydrogen production, *Energy Rep.*, 2022, **8**, 13793–13813.

18 P. Nikolaidis and A. Poullikkas, A comparative overview of hydrogen production processes, *Renewable Sustainable Energy Rev.*, 2017, **67**, 597–611.

19 M. Yu, K. Wang and H. Vredenburg, Insights into low-carbon hydrogen production methods: Green, blue and aqua hydrogen, *Int. J. Hydrogen Energy*, 2021, **46**, 21261–21273.

20 X. Shi, L. Cai, M. Ma, X. Zheng and J. H. Park, General Characterization Methods for Photoelectrochemical Cells for Solar Water Splitting, *ChemSusChem*, 2015, **8**, 3192–3203.

21 J. Joy, J. Mathew and S. C. George, Nanomaterials for photoelectrochemical water splitting – review, *Int. J. Hydrogen Energy*, 2018, **43**, 4804–4817.

22 M. R. Nellist, F. A. L. Laskowski, F. Lin, T. J. Mills and S. W. Boettcher, Semiconductor–Electrocatalyst Interfaces: Theory, Experiment, and Applications in Photoelectrochemical Water Splitting, *Acc. Chem. Res.*, 2016, **49**, 733–740.

23 Z. Bai and Y. Zhang, A Cu_2O/Cu_2S–ZnO/CdS tandem photoelectrochemical cell for self-driven solar water splitting, *J. Alloys Compd.*, 2017, **698**, 133–140.

24 J. Miao, H. B. Yang, S. Y. Khoo and B. Liu, Electrochemical fabrication of ZnO–CdSe core–shell nanorod arrays for efficient photoelectrochemical water splitting, *Nanoscale*, 2013, **5**, 11118–11124.

25 S. Masudy-Panah, R. Siavash Moakhar, C. S. Chua, H. R. Tan, T. I. Wong, D. Chi and G. K. Dalapati, Nanocrystal Engineering of Sputter-Grown CuO Photocathode for Visible-Light-Driven Electrochemical Water Splitting, *ACS Appl. Mater. Interfaces*, 2016, **8**, 1206–1213.

26 R. Siavash Moakhar, S. M. Hosseini-Hosseinabad, S. Masudy-Panah, A. Seza, M. Jalali, H. Fallah-Arani, F. Dabir, S. Gholipour, Y. Abdi, M. Bagheri-Hariri, N. Riahi-Noori, Y.-F. Lim, A. Hagfeldt and M. Saliba, Photoelectrochemical Water-Splitting Using CuO-Based Electrodes for Hydrogen Production: A Review, *Adv. Mater.*, 2021, **33**, 2007285.

27 M. Klusáčková, R. Nebel, P. Krtil, H. Krýsová, R. K. Pittkowski and K. M. Macounová, Photo-electrochemical activity and selectivity of nanocrystalline $BaTiO_3$ electrodes in water oxidation, *Electrochem. Sci. Adv.*, 2021, **1**, e2000005.

28 S. Assavachin and F. E. Osterloh, Ferroelectric Polarization in $BaTiO_3$ Nanocrystals Controls Photoelectrochemical Water Oxidation and Photocatalytic Hydrogen Evolution, *J. Am. Chem. Soc.*, 2023, **145**, 18825–18833.

29 X. Yao, D. Wang, X. Zhao, S. Ma, P. S. Bassi, G. Yang, W. Chen, Z. Chen and T. Sritharan, Scale-Up of $BiVO_4$ Photoanode for Water Splitting in a Photoelectrochemical Cell: Issues and Challenges, *Energy Technol.*, 2018, **6**, 100–109.

30 M. Guo and G. Ma, Alteration of onset potentials of Rh-doped $SrTiO_3$ electrodes for photoelectrochemical water splitting, *J. Catal.*, 2020, **391**, 241–246.

31 K. Arifin, R. M. Yunus, L. J. Minggu and M. B. Kassim, Improvement of TiO_2 nanotubes for photoelectrochemical water splitting: Review, *Int. J. Hydrogen Energy*, 2021, **46**, 4998–5024.

32 Z. Yu, H. Liu, M. Zhu, Y. Li and W. Li, Interfacial Charge Transport in 1D TiO_2 Based Photoelectrodes for Photoelectrochemical Water Splitting, *Small*, 2021, **17**, 1903378.

33 S. Franz, H. Arab, G. L. Chiarello, M. Bestetti and E. Selli, Single-Step Preparation of Large Area TiO_2 Photoelectrodes for Water Splitting, *Adv. Energy Mater.*, 2020, **10**, 2000652.

34 W.-H. Cheng, M. H. Richter, M. M. May, J. Ohlmann, D. Lackner, F. Dimroth, T. Hannappel, H. A. Atwater and H.-J. Lewerenz, Monolithic Photoelectrochemical Device for Direct Water Splitting with 19% Efficiency, *ACS Energy Lett.*, 2018, **3**, 1795–1800.

35 Y. Zhao, S. Balasubramanyam, R. Sinha, R. Lavrijsen, M. A. Verheijen, A. A. Bol and A. Bieberle-Hütter, Physical and Chemical Defects in WO_3 Thin Films and Their Impact on Photoelectrochemical Water Splitting, *ACS Appl. Energy Mater.*, 2018, **1**, 5887–5895.

36 R. Zhang, F. Ning, S. Xu, L. Zhou, M. Shao and M. Wei, Oxygen vacancy engineering of WO_3 toward largely enhanced photoelectrochemical water splitting, *Electrochim. Acta*, 2018, **274**, 217–223.

37 S. S. Kalanur, I.-H. Yoo, K. Eom and H. Seo, Enhancement of photoelectrochemical water splitting response of WO_3 by Means of Bi doping, *J. Catal.*, 2018, **357**, 127–137.

38 D. Dworschak, C. Brunnhofer and M. Valtiner, Photocorrosion of ZnO Single Crystals during Electrochemical Water Splitting, *ACS Appl. Mater. Interfaces*, 2020, **12**, 51530–51536.
39 J. Kegel, I. M. Povey and M. E. Pemble, Zinc oxide for solar water splitting: A brief review of the material's challenges and associated opportunities, *Nano Energy*, 2018, **54**, 409–428.
40 Z. Kang, H. Si, S. Zhang, J. Wu, Y. Sun, Q. Liao, Z. Zhang and Y. Zhang, Interface Engineering for Modulation of Charge Carrier Behavior in ZnO Photoelectrochemical Water Splitting, *Adv. Funct. Mater.*, 2019, **29**, 1808032.
41 S. Guo, X. Zhao, W. Zhang and W. Wang, Optimization of electrolyte to significantly improve photoelectrochemical water splitting performance of ZnO nanowire arrays, *Mater. Sci. Eng., B*, 2018, **227**, 129–135.
42 S. K. Saraswat, D. D. Rodene and R. B. Gupta, Recent advancements in semiconductor materials for photoelectrochemical water splitting for hydrogen production using visible light, *Renewable Sustainable Energy Rev.*, 2018, **89**, 228–248.
43 W. Yang, R. R. Prabhakar, J. Tan, S. D. Tilley and J. Moon, Strategies for enhancing the photocurrent, photovoltage, and stability of photoelectrodes for photoelectrochemical water splitting, *Chem. Soc. Rev.*, 2019, **48**, 4979–5015.
44 R.-T. Gao, N. T. Nguyen, T. Nakajima, J. He, X. Liu, X. Zhang, L. Wang and L. Wu, Dynamic semiconductor-electrolyte interface for sustainable solar water splitting over 600 hours under neutral conditions, *Sci. Adv.*, 2023, **9**, eade4589.
45 T. T. Hien, N. D. Quang, C. Kim and D. Kim, Energy diagram analysis of photoelectrochemical water splitting process, *Nano Energy*, 2019, **57**, 660–669.
46 X. Liu, J. Chi, B. Dong and Y. Sun, Recent Progress in Decoupled H_2 and O_2 Production from Electrolytic Water Splitting, *ChemElectroChem*, 2019, **6**, 2157–2166.
47 B. Yao, J. Zhang, X. Fan, J. He and Y. Li, Surface Engineering of Nanomaterials for Photo-Electrochemical Water Splitting, *Small*, 2019, **15**, 1803746.
48 J.-W. Lee, K.-H. Cho, J.-S. Yoon, Y.-M. Kim and Y.-M. Sung, Photoelectrochemical water splitting using one-dimensional nanostructures, *J. Mater. Chem. A*, 2021, **9**, 21576–21606.
49 T. Butburee, Y. Bai, H. Wang, H. Chen, Z. Wang, G. Liu, J. Zou, P. Khemthong, G. Q. M. Lu and L. Wang, 2D Porous TiO_2 Single-Crystalline Nanostructure Demonstrating High Photo-Electrochemical Water Splitting Performance, *Adv. Mater.*, 2018, **30**, 1705666.
50 T. S. Atabaev, Plasmon-enhanced solar water splitting with metal oxide nanostructures: A brief overview of recent trends, *Front. Mater. Sci.*, 2018, **12**, 207–213.
51 J. Kwon, H. Cho, J. Jung, H. Lee, S. Hong, J. Yeo, S. Han and S. H. Ko, ZnO/CuO/M (M = Ag, Au) Hierarchical Nanostructure by Successive Photoreduction Process for Solar Hydrogen Generation, *Nanomaterials*, 2018, **8**, 323.
52 M. Chandra and D. Pradhan, Engineering the Morphology and Crystal Phase of 3 D Hierarchical TiO_2 with Excellent Photochemical and Photoelectrochemical Solar Water Splitting, *ChemSusChem*, 2020, **13**, 3005–3016.
53 Z. Wang, H. Zhu, W. Tu, X. Zhu, Y. Yao, Y. Zhou and Z. Zou, Host/Guest Nanostructured Photoanodes Integrated with Targeted Enhancement Strategies for Photoelectrochemical Water Splitting, *Adv. Sci.*, 2022, **9**, 2103744.
54 A. Baptista, F. Silva, J. Porteiro, J. Míguez and G. Pinto, Sputtering Physical Vapour Deposition (PVD) Coatings: A Critical Review on Process Improvement and Market Trend Demands, *Coatings*, 2018, **8**, 402.
55 Y. Deng, W. Chen, B. Li, C. Wang, T. Kuang and Y. Li, Physical vapor deposition technology for coated cutting tools: A review, *Ceram. Int.*, 2020, **46**, 18373–18390.
56 S. Limwichean, N. Kasayapanand, C. Ponchio, H. Nakajima, V. Patthanasettakul, P. Eiamchai, G. Meng and M. Horprathum, Morphology-controlled fabrication of nanostructured WO_3 thin films by magnetron sputtering with glancing angle deposition for enhanced efficiency photoelectrochemical water splitting, *Ceram. Int.*, 2021, **47**, 34455–34462.
57 J. Yadav and J. P. Singh, WO_3/Ag_2S type-II hierarchical heterojunction for improved charge carrier separation and photoelectrochemical water splitting performance, *J. Alloys Compd.*, 2022, **925**, 166684.
58 T. Higashi, Y. Sasaki, Y. Kawase, H. Nishiyama, M. Katayama, K. Takanabe and K. Domen, Surface-Modified Ta_3N_5 Photoanodes for Sunlight-Driven Overall Water Splitting by Photoelectrochemical Cells, *Catalysts*, 2021, **11**, 584.
59 L. Sun, G. Yuan, L. Gao, J. Yang, M. Chhowalla, M. H. Gharahcheshmeh, K. K. Gleason, Y. S. Choi, B. H. Hong and Z. Liu, Chemical vapour deposition, *Nat. Rev. Methods Primers*, 2021, **1**, 5.
60 J. Jiang, N. Li, J. Zou, X. Zhou, G. Eda, Q. Zhang, H. Zhang, L.-J. Li, T. Zhai and A. T. S. Wee, Synergistic additive-mediated CVD growth and chemical modification of 2D materials, *Chem. Soc. Rev.*, 2019, **48**, 4639–4654.
61 J. Schmitz, Low temperature thin films for next-generation microelectronics (invited), *Surf. Coat. Technol.*, 2018, **343**, 83–88.
62 I. Bretos, R. Jiménez, J. Ricote and M. L. Calzada, Low-temperature crystallization of solution-derived metal oxide thin films assisted by chemical processes, *Chem. Soc. Rev.*, 2018, **47**, 291–308.
63 H. Xin and W. Li, A review on high throughput roll-to-roll manufacturing of chemical vapor deposition graphene, *Appl. Phys. Rev.*, 2018, **5**, 031105.
64 S. Swathi, E. S. Babu, R. Yuvakkumar, G. Ravi, A. Chinnathambi, S. A. Alharbi and D. Velauthapillai, Branched and unbranched ZnO nanorods grown *via* chemical vapor deposition for photoelectrochemical water-splitting applications, *Ceram. Int.*, 2021, **47**, 9785–9790.
65 S. Swathi, R. Yuvakkumar, G. Ravi, E. S. Babu, D. Velauthapillai and S. A. Alharbi, Morphological exploration of chemical vapor–deposited P-doped ZnO nanorods for efficient photoelectrochemical water splitting, *Ceram. Int.*, 2021, **47**, 6521–6527.

66 K. C. Lau, M. L. Ooi, Z. X. Ooi, R. C. S. Wong, Z. L. Choong, M. Mazhar and B. T. Goh, Fabrication of Fe-Doped Molybdenum Multisulfide MoS_2/Mo_2S_3 Thin Film *Via* Aerosol-Assisted Chemical Vapor Deposition (AACVD) for Photoelectrochemical (PEC) Water Splitting, *Electrocatalysis*, 2022, **13**, 182–194.

67 L. Jozwiak, J. Balcerzak and J. Tyczkowski, Plasma-Deposited Ru-Based Thin Films for Photoelectrochemical Water Splitting, *Catalysts*, 2020, **10**, 278.

68 Y.-F. Zhang, Y.-K. Zhu, C.-X. Lv, S.-J. Lai, W.-J. Xu, J. Sun, Y.-Y. Sun and D.-J. Yang, Enhanced visible-light photoelectrochemical performance *via* chemical vapor deposition of Fe_2O_3 on a WO_3 film to form a heterojunction, *Rare Met.*, 2020, **39**, 841–849.

69 R. A. Ovanesyan, E. A. Filatova, S. D. Elliott, D. M. Hausmann, D. C. Smith and S. Agarwal, Atomic layer deposition of silicon-based dielectrics for semiconductor manufacturing: Current status and future outlook, *J. Vac. Sci. Technol., A*, 2019, **37**, 060904.

70 Y. Hu, J. Lu and H. Feng, Surface modification and functionalization of powder materials by atomic layer deposition: a review, *RSC Adv.*, 2021, **11**, 11918–11942.

71 J. Zhang, Y. Li, K. Cao and R. Chen, Advances in Atomic Layer Deposition, *Nanomanuf. Metrol.*, 2022, **5**, 191–208.

72 T. Justin Kunene, L. Kwanda Tartibu, K. Ukoba and T.-C. Jen, Review of atomic layer deposition process, application and modeling tools, *Mater. Today: Proc.*, 2022, **62**, S95–S109.

73 Y. Wang, S. Cao, Y. Huan, T. Nie, Z. Ji, Z. Bai, X. Cheng, J. Xi and X. Yan, The effect of composite catalyst on Cu_2O/TiO_2 heterojunction photocathodes for efficient water splitting, *Appl. Surf. Sci.*, 2020, **526**, 146700.

74 A. Song, P. Bogdanoff, A. Esau, I. Y. Ahmet, I. Levine, T. Dittrich, T. Unold, R. van de Krol and S. P. Berglund, Assessment of a W:$BiVO_4$–$CuBi_2O_4$ Tandem Photoelectrochemical Cell for Overall Solar Water Splitting, *ACS Appl. Mater. Interfaces*, 2020, **12**, 13959–13970.

75 K.-I. Liu and T.-P. Perng, Fabrication of Flower-Like WO_3/TiO_2 Core–Shell Nanoplates by Atomic Layer Deposition for Improved Photoelectrochemical Water-Splitting Activity, *ACS Appl. Energy Mater.*, 2020, **3**, 4238–4244.

76 X. Feng, L. Sun, W. Wang, Y. Zhao and J.-W. Shi, Construction of CdS@ZnO core–shell nanorod arrays by atomic layer deposition for efficient photoelectrochemical H_2 evolution, *Sep. Purif. Technol.*, 2023, **324**, 124520.

77 B. Alfakes, C. Garlisi, J. Villegas, A. Al-Hagri, S. Tamalampudi, N. S. Rajput, J.-Y. Lu, E. Lewin, J. Sá, I. Almansouri, G. Palmisano and M. Chiesa, Enhanced photoelectrochemical performance of atomic layer deposited Hf-doped ZnO, *Surf. Coat. Technol.*, 2020, **385**, 125352.

78 H. Park, J. J. Park, P.-D. Bui, H. Yoon, C. P. Grigoropoulos, D. Lee and S. H. Ko, Laser-Based Selective Material Processing for Next-Generation Additive Manufacturing, *Adv. Mater.*, 2023, 2307586.

79 S. Song, H. Hong, K. Y. Kim, K. K. Kim, J. Kim, D. Won, S. Yun, J. Choi, Y.-I. Ryu, K. Lee, J. Park, J. Kang, J. Bang, H. Seo, Y.-C. Kim, D. Lee, H. Lee, J. Lee, S.-W. Hwang, S. H. Ko, H. Jeon and W. Lee, Photothermal Lithography for Realizing a Stretchable Multilayer Electronic Circuit Using a Laser, *ACS Nano*, 2023, **17**, 21443–21454.

80 J. Shin, J. Ko, S. Jeong, P. Won, Y. Lee, J. Kim, S. Hong, N. L. Jeon and S. H. Ko, Monolithic digital patterning of polydimethylsiloxane with successive laser pyrolysis, *Nat. Mater.*, 2021, **20**, 100–107.

81 S. Song, S.-H. Um, J. Park, I. Ha, J. Lee, S. Kim, H. Lee, C.-H. Cheon, S. H. Ko, Y.-C. Kim and H. Jeon, Rapid Synthesis of Multifunctional Apatite *via* the Laser-Induced Hydrothermal Process, *ACS Nano*, 2022, **16**, 12840–12851.

82 P. You, G. Li, G. Tang, J. Cao and F. Yan, Ultrafast laser-annealing of perovskite films for efficient perovskite solar cells, *Energy Environ. Sci.*, 2020, **13**, 1187–1196.

83 Y. Rho, K. Lee, L. Wang, C. Ko, Y. Chen, P. Ci, J. Pei, A. Zettl, J. Wu and C. P. Grigoropoulos, A laser-assisted chlorination process for reversible writing of doping patterns in graphene, *Nat. Electron.*, 2022, **5**, 505–510.

84 S. Hong, H. Lee, J. Yeo and S. H. Ko, Digital selective laser methods for nanomaterials: From synthesis to processing, *Nano Today*, 2016, **11**, 547–564.

85 M. Kölbach, K. Harbauer, K. Ellmer and R. van de Krol, Elucidating the Pulsed Laser Deposition Process of $BiVO_4$ Photoelectrodes for Solar Water Splitting, *J. Phys. Chem. C*, 2020, **124**, 4438–4447.

86 S. Ye, W. Shi, Y. Liu, D. Li, H. Yin, H. Chi, Y. Luo, N. Ta, F. Fan, X. Wang and C. Li, Unassisted Photoelectrochemical Cell with Multimediator Modulation for Solar Water Splitting Exceeding 4% Solar-to-Hydrogen Efficiency, *J. Am. Chem. Soc.*, 2021, **143**, 12499–12508.

87 H. Lu, S. Fang, J. Hu, B. Chen, R. Zhao, H. Li, C. M. Li and J. Ye, Fabrication of a TiO_2/Fe_2O_3 Core/Shell Nanostructure by Pulse Laser Deposition toward Stable and Visible Light Photoelectrochemical Water Splitting, *ACS Omega*, 2020, **5**, 19861–19867.

88 H. Kong, J. Kwon, D. Paeng, W. J. Jung, S. Ghimire, J. Dho, J.-H. Yoo, S. Hong, J. Jung, J. Shin, C. P. Grigoropoulos, S. H. Ko and J. Yeo, Laser-Induced Crystalline-Phase Transformation for Hematite Nanorod Photoelectrochemical Cells, *ACS Appl. Mater. Interfaces*, 2020, **12**, 48917–48927.

89 D. Wang, S. Gao, C. Li, Y. Wang, H. Zhu, Y. Liu and X. Zhang, Pulse laser annealing activates titanium-doped hematite photoanodes for photoelectrochemical water oxidation, *Appl. Surf. Sci.*, 2020, **528**, 147062.

90 K. Grochowska, Z. Molenda, J. Karczewski, J. Bachmann, K. Darowicki, J. Ryl and K. Siuzdak, Laser induced formation of copper species over TiO_2 nanotubes towards enhanced water splitting performance, *Int. J. Hydrogen Energy*, 2020, **45**, 19192–19205.

91 M. Qiao, J. Yan, L. Qu, B. Zhao, J. Yin, T. Cui and L. Jiang, Femtosecond Laser Induced Phase Transformation of TiO_2 with Exposed Reactive Facets for Improved Photoelectrochemistry Performance, *ACS Appl. Mater. Interfaces*, 2020, **12**, 41250–41258.

92 H. Kong, S. Hwang, J. Lee, S. W. Park, Y.-S. Han and J. Yeo, Laser-Induced Photoreduction for Selective Tuning of the Oxidation State and Crystal Structure of Hematite Nanorods, *J. Phys. Chem. C*, 2021, **125**, 17918–17928.

93 H. Kong, H. Yang, J.-S. Park, W.-S. Chae, H. Y. Kim, J. Park, J. H. Lee, S. Y. Choi, M. Park, H. Kim, Y. Song, H. Park and J. Yeo, Spatial Control of Oxygen Vacancy Concentration in Monoclinic WO_3 Photoanodes for Enhanced Solar Water Splitting, *Adv. Funct. Mater.*, 2022, **32**, 2204106.

94 M. Barawi, M. Gomez-Mendoza, F. E. Oropeza, G. Gorni, I. J. Villar-Garcia, S. Giménez, V. A. de la Peña O'Shea and M. García-Tecedor, Laser-Reduced $BiVO_4$ for Enhanced Photoelectrochemical Water Splitting, *ACS Appl. Mater. Interfaces*, 2022, **14**, 33200–33210.

95 T. Nakajima, T. Nakamura, K. Shinoda and T. Tsuchiya, Rapid formation of black titania photoanodes: pulsed laser-induced oxygen release and enhanced solar water splitting efficiency, *J. Mater. Chem. A*, 2014, **2**, 6762–6771.

96 H. Y. Kim, H. Kong, J. H. Kim, W.-G. Yang, H. Lee, S. Ko, H. J. Lee, G. Piao, H. Park, W.-S. Chae and J. Yeo, Laser-induced deposition of Ni, Co-doped FeOOH cocatalysts on WO_3 photoanodes and elucidating their roles in water oxidation in terms of carrier dynamics, *J. Mater. Chem. A*, 2023, **11**, 4598–4607.

97 F. Li, J. Jian, J. Zou, S. Wang, Z. Zhang, L. Jia, M. Fu, X. Guan and H. Wang, Bulk embedding of Ti-defected TiO_2 nano-heterointerfaces in hematite photoanode for boosted photoelectrochemical water splitting, *Chem. Eng. J.*, 2023, **473**, 145254.

98 F. Li, J. Jian, S. Wang, Z. Zhang, L. Jia, X. Guan, Y. Xu and H. Wang, TiO_2 passivation layers with laser derived p–n heterojunctions enable boosted photoelectrochemical performance of α-Fe_2O_3 photoanodes, *Chem. Eng. J.*, 2023, **461**, 141872.

99 J. Jian, Y. Xu, X. Yang, W. Liu, M. Fu, H. Yu, F. Xu, F. Feng, L. Jia, D. Friedrich, R. van de Krol and H. Wang, Embedding laser generated nanocrystals in $BiVO_4$ photoanode for efficient photoelectrochemical water splitting, *Nat. Commun.*, 2019, **10**, 2609.

100 J. Jian, S. Wang, Q. Ye, F. Li, G. Su, W. Liu, C. Qu, F. Liu, C. Li, L. Jia, A. A. Novikov, V. A. Vinokurov, D. H. S. Harvey, D. Shchukin, D. Friedrich, R. van de Krol and H. Wang, Activating a Semiconductor–Liquid Junction *via* Laser-Derived Dual Interfacial Layers for Boosted Photoelectrochemical Water Splitting, *Adv. Mater.*, 2022, **34**, 2201140.

101 T. Sharifi, T. Mohammadi, M. M. Momeni, H. Kusic, M. Kraljic Rokovic, A. Loncaric Bozic and Y. Ghayeb, Influence of Photo-Deposited Pt and Pd onto Chromium Doped TiO_2 Nanotubes in Photo-Electrochemical Water Splitting for Hydrogen Generation, *Catalysts*, 2021, **11**, 212.

102 P. Qiu, F. Li, H. Zhang, S. Wang, Z. Jiang and Y. Chen, Photoelectrochemical performance of α-Fe_2O_3@NiOOH fabricated with facile photo-assisted electrodeposition method, *Electrochim. Acta*, 2020, **358**, 136847.

103 T. Wang, X. Long, S. Wei, P. Wang, C. Wang, J. Jin and G. Hu, Boosting Hole Transfer in the Fluorine-Doped Hematite Photoanode by Depositing Ultrathin Amorphous FeOOH/CoOOH Cocatalysts, *ACS Appl. Mater. Interfaces*, 2020, **12**, 49705–49712.

104 X. Zhao, Y. Rui, Y. Bai, J. Huang, H. She, J. Peng and Q. Wang, The PEC performance of $BiVO_4$ was enhanced by preparing the CoFeBi/$BiVO_4$ photoanode using an ultrafast photoassisted electrodeposition method, *CrystEngComm*, 2023, **25**, 6677–6684.

105 K. Tian, L. Wu, H. Chai, L. Gao, M. Wang, H. Niu, L. Chen and J. Jin, Enhancement of charge separation and hole utilization in a $Ni_2P_2O_7$-Nd-$BiVO_4$ photoanode for efficient photoelectrochemical water oxidation, *J. Colloid Interface Sci.*, 2023, **644**, 124–133.

106 M. A. Mahadik, H. H. Lee, W.-S. Chae, M. Cho and J. S. Jang, Energy-efficient photoelectrochemical water splitting and degradation of organic dyes over microwave-assisted WO_3 nanosheets/W foil with rapid charge transport, *Sol. Energy Mater. Sol. Cells*, 2022, **246**, 111939.

107 T. S. Koh, P. Anushkkaran, W.-S. Chae, H. H. Lee, S. H. Choi and J. S. Jang, Gradient Si- and Ti-doped Fe_2O_3 hierarchical homojunction photoanode for efficient solar water splitting: Effect of facile microwave-assisted growth of Si-FeOOH on Ti-FeOOH nanocorals, *J. Energy Chem.*, 2023, **77**, 27–37.